AuPS/ASB Meeting - Canberra 2005

1615 - Poster Session, Afternoon Tea and Drinks

Wednesday 28 September 2005

Effects of gadolinium and static magnetic fields on MscL channel activity

E. Petrov, Z.-W. Liu and B. Martinac, School of Biomedical Sciences, University of Queensland, St Lucia, Queensland 4072 Australia.

All biological tissues are highly penetrable for static magnetic fields (SMF). There are a number of hypotheses concerning the cellular and/or subcellular target of these fields. One possibility is that they target the cell membrane. It was shown that applying a SMF of 80 mT affected the open probability (P_o) and gating of the bacterial **M**echano**s**ensitive **c**hannel of **L**arge conductance (MscL) reconstituted into liposomes (Hughes *et al.*, 2005). Since phospholipid molecules possess diamagnetic anisotropy (Rosen, 2003), the SMF effect on MscL could originate from the reorientation of the lipid molecules perpendicularly to the direction of the magnetic field. Taking into account that thousands of phospholipid molecules form well ordered arrays in the bilayer the effect of SMF thus becomes amplified affecting the embedded MscL protein. Another possible effect of SMF could be *via* membrane-bound ions, such as Ca^{2+} (Del Moral & Azanza, 1994). To test this hypothesis we examined if SMF could modulate the ability of Gd^{3+} ions (non-specific blocker of mechanosensitive channels (Hamill & McBride, 1996)) to inhibit MscL gating, since Gd^{3+} ions interact with phospholipid molecules in a similar way as Ca^{2+} ions (Ermakov *et al.*, 2001).

Single channel patch-clamp experiments were carried out using the MscL channels reconstituted into liposomes and effect of Gd^{3+} on MscL activity was recorded. The results showed that Gd^{3+}, in a dose-dependent manner, caused an increase in the negative pressure required to open the MscL channels. 50 μM Gd^{3+} in the bath partially blocked the MscL channel, whereas 400 μM Gd^{3+} blocked the channels completely. Gd^{3+} also prolonged the duration of the single channel openings by decreasing the frequency of the channel opening and reducing channel flickering.

Next we studied the effect of SMF on the MscL activity and MscL block by Gd^{3+}. Negative pressures of 40-50 mmHg were required to stretch liposome patches and activate the MscL channels. Only patches were examined which exhibited stable channel activity during the initial 5-7 minutes of an experiment. A rare-earth NdFeB magnet was positioned at a distance of 2 mm from the tip of the pipette. The estimated strength of SMF was 400 mT. Application of the SMF had a two-fold effect on the channel activity: (1) a decrease of the open probability NP_o (N, unknown number of channels in a patch) during application of the SMF to 70.6±8.3% (mean±S.E., n=10) of the initial steady-state level before the application of SMF; and (2) an increase of NP_o upon removal of the SMF to 119.0±10.8% (n=10). The effects of the SMF were slowly developing over approximately 10 minutes upon application /release of the SMF. The time-dependence of the SMF effect may be explained by formation and destruction of ordered phospholipid clusters in the bilayer. Variability in the extent of the observed effects in our experiments might be due to the fact that the patch membrane is not flat when suction is applied to the pipette (Sukharev *et al.*, 1999), so that the peripheral and central parts of a patch are at different angles to the SMF vector. In most of the examined patches a partial blockade of the MscL activity by 50 μM of Gd^{3+} increased in the presence of SMF. After removal of SMF the channel activity recovered to the previous level and often increased further regardless of the presence of Gd^{3+} ions. In some patches the channel activity did not increase after the removal of SMF, but had already done so in its presence. Our results suggest that ordering of phospholipid molecules in the bilayer by SMF could cause a displacement of Gd^{3+} ions bound to phospholipid molecules due to the electrostatic repulsion between the ions, which resulted in reduction of the MscL channel block by Gd^{3+}.

Del Moral, A. & Azanza, M.J. (1994) *Progress in Neurobiology* **44**, 517-601.
Ermakov, Y.A., Averbakh, A.Z., Yusipovich, A.I. & Sukharev, S. I. (2001) *Biophysical Journal* **80**, 1851-1862.
Hamill, O.P. & McBride, D.W. Jr. (1996) *Pharmacological Reviews* **48**, 231-252.
Hughes, S., El Haj, A.J., Dobson, J. & Martinac, B. (2005) *European Biophysics Journal* (in press).
Rosen, A.D. (2003) *Cell Biochemistry and Biophysics* **39**, 163-173. Sukharev, S.I., Sigurdson, W.J., Kung, C. & Sachs F. (1999) *Journal of General Physiology*. **113**, 525-540.

Conformational changes involved in MscL channel gating measured using FRET spectroscopy

B. Corry[1], P. Rigby[2] and B. Martinac[3], [1]Chemistry, School of Biomedical, Biomolecular and Chemical Science, [2]Biomedical Imaging and Analysis Facility and [3]School of Medicine and Pharmacology, The University of Western Australia, Crawley, WA 6009, Australia.

Transmembrane channels facilitate the movement of small molecules and ions across cell membranes. Obtaining detailed structural information about such proteins has been difficult, due not only to the complications of crystallisation, but also because they adopt multiple conformational states that are not easy to probe with static x-ray images. We demonstrate that fluorescence resonance energy transfer spectroscopy (FRET) is a powerful tool for *in situ* structural analysis of multimeric membrane proteins by measuring the conformational changes involved in gating the mechanosensitive ion channel MscL.

MscL channels act as safety valves in bacterial cells, opening wide pores to prevent cell death during hypo-osmotic stress. The MscL protein monomers are fluorescently labelled by randomly attaching AlexaFluor 488 (AF488) and AlexaFluor 568 (AF568) to a single cysteine residue introduced *via* site directed mutagenesis. As the channel protein is a pentamer, this mutation introduces five identical cysteine sites each equally likely to be occupied by AF488 or AF568. The protein is reconstituted into artificial phosphatidylcholine liposomes and imaged in a laser scanning confocal microscope. The channels are normally closed in their resting state, but may be forced into the open conformational state with the addition of lysophosphatidylcholine (LPC) which inserts in the outer layer of the liposome membrane bilayer promoting membrane curvature and/or a change in the transbilayer pressure profile, thus leading to channel opening.

The liposomes are imaged in both AF488 (donor) and AF568 (acceptor) emission bands before and after bleaching of the acceptor AF568. The intensity of the AF488 donor emission increases after bleaching indicating FRET is taking place.

The proportion of energy being transferred from the donor to the acceptor is then related to the pentamer radius in both the closed and open channels using a Monte-Carlo ensemble analysis program. This accounts for each channel protein containing a random mix of five donors and acceptors and the fact that energy transfer could arise between fluorophores attached to different proteins.

As illustrated schematically in the figure, we find that the diameter of the fluorescently labelled MscL channel increases by 16Å upon activation, creating a large pore and representing one of the largest known conformational changes in membrane proteins.

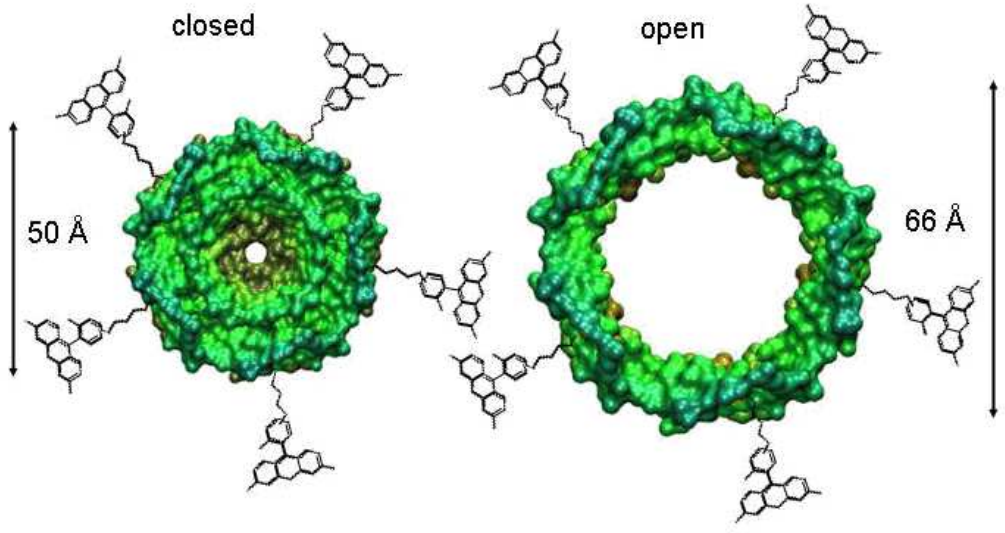

C-terminal charged cluster of the mechanosensitive channel MscL, RKKEE, functions as a pH sensor

Anna Kloda and Boris Martinac, School of Biomedical Sciences, University of Queensland, Brisbane, Queensland 4072 Australia.

A highly conserved cluster of charged residues, RKKEE, located within the C-terminus of the bacterial mechanosensitive channel MscL is essential for the channel gating. The mutated protein lacking these amino acid residues is not functional (Häse *et al.*, 1997). This structural motif is a part of a cytoplasmic helix and is proposed to serve as a stabilizing element of the closed configuration of the MscL channel (Perozo *et al.*, 2001). The crystal structure of MscL was obtained at low pH showing the channel in its closed state (Chang *et al.*, 1998). In the crystal structure the charged residues are facing each other inside the C-terminal helical bundle. However an independent study of the channel closed structure (Perozo *et al.*, 2001) shows that at neutral pH these residues are outwardly oriented facing the aqueous medium. This suggests that the orientation of the C-terminal helices relative to the aqueous medium is pH dependent. Thus, it is possible that the RKKEE cluster functions as a pH sensor. In the present study we examined the effects of pH as well as of charge reversal and substitution within the RKKEE cluster on mechanosensitivity of *E. coli* MscL reconstituted into liposomes using the patch-clamp technique.

Charge reversal mutations did not affect the free energy of activation or activation pressure of the channel (ΔG_0 = 15.8 kT, $p_{1/2}$ = 76.3 mmHg and ΔG_0 = 16.4 kT, $p_{1/2}$ = 84.2 mmHg) for the RKKEE wild type and the EEKKR mutant respectively. Protonation of E107 and E108 residues, achieved by decreasing the experimental pH or replacement of negative charges by glutamine, significantly increased free energy of activation for the MscL channel due to an increase in activation pressure $p_{1/2}$ (ΔG_0 = 26.9 kT, $p_{1/2}$ = 120.2 mmHg for wild type MscL at pH 5.5 and ΔG_0 = 26.1 kT, $p_{1/2}$ = 130.3 mmHg for the RKKQQ mutant channel at pH 7.0). A similar increase in ΔG_0 was observed when positive charges were substituted by glutamine (ΔG_0 = 23.8 kT, $p_{1/2}$ = 118.6 mmHg at pH 7.0) or the overall charge of the cluster was neutralized by increasing experimental pH of the RKKQQ mutant (ΔG_0 = 25.7 kT, $p_{1/2}$ = 124.0 pH 9.5). Interestingly, protonation of the positively charged residues of the RKKQQ mutant by lowering the experimental pH to 5.5 resulted in $p_{1/2}$ (89.0 mmHg) and ΔG_0 (13.0 kT) comparable to the wild-type MscL at physiological pH of 7.0 suggesting the importance of the preservation of the total charge of the cluster. Our data indicate that the RKKEE charged cluster acts as a pH sensor that regulates the stability of the cytoplasmic helix. Our data further suggest that, in contrast to the gating model proposed by Anishkin *et al.* (2003) the cytoplasmic helix is not only functioning as a size-exclusion filter but also substantially influences channel gating.

Anishkin, A., Gendel, V., Sharifi, N.A., Chiang, C.S., Shirinian, L., Guy, H.R. & Sukharev, S. (2003) *Journal of General Physiology*, 121, 227-244.

Chang, G., Spencer, R.H., Lee, A.T., Barclay, M.T. & Rees, D.C. (1998) *Science*, 282, 2220-2226.

Häse, C.C., Ledain, A.C. & Martinac, B. (1997) *Journal of Membrane Biology*, 157, 17-25.

Perozo, E., Kloda, A., Cortes, D.M. & Martinac, B. (2001) *Journal of General Physiology*, 118, 193-205.

The effects of eriochrome cyanine R on the mechanosensitive channels of *E. coli*

T. Nguyen[1,2], B. Clare[2], L. Hool[2] and B. Martinac[3], [1]School of Medicine and Pharmacology, University of Western Australia, WA 6009, Australia[2], School of Biomedical, Biomolecular and Chemical Sciences, University of Western Australia, WA 6009, Australia and [3]School of Biomedical Sciences, University of Queensland, QLD 4072, Australia.

The existence and characteristics of the mechanosensitive channel of large conductance (MscL) and small conductance (MscS) of *E.coli* have been well documented and extensively studied (Sukharev *et al.*, 1997). MscL and MscS have been found to play an important role in osmoregulation and the two channels are capable of compensating the absence of each other (Berrier *et al.*, 1992; Levina *et al.*, 1999). Though similar in physiological function, the channels differ somewhat in structure and characteristic. The *MscL* gene comprises of 136 amino acid residues amounting to a 15-kDa protein (Sukharev *et al.*, 1994) to form a homopentamer (Chang *et al.*, 1998). Whereas, MscS, is a 286-residue membrane protein with its 3D structure revealing a homoheptamer (Bass *et al.*, 2002). MscS is gated at pressures approximately half of which MscL is activated and has a conductance of ~1nS (Martinac *et al.*, 1987; Sukharev *et al.*, 1993) compared to MscL conductance of ~3nS (Sukharev *et al.*, 1994).

We have previously shown that parabens, which are food and cosmetic preservatives, were able to spontaneously activate MscL reconstituted in liposomes and MscS in giant spheroplasts, and also increased the mechanosensitivity of MscL (Nguyen *et al.*, 2005). Our studies therefore, broaden to other compounds which would bind to the MscL gate with greater affinity than parabens. Based on our *in-silico* data, eriochrome cyanine R bound to the MscL channel gate with a Gibbs free energy of -47.03kJ mol^{-1} which is a much lower value than that of parabens, indicating a greater affinity to the channel.

The patch-clamp studies with eriochrome cyanine R were shown to complement *in-silico* results with spontaneous MscL activity observed in 78% of the patches. The Boltzmann distribution curve of MscL in the presence of eriochrome cyanine R was markedly shifted to the left of the control curve and the Boltzmann parameters namely, α, $p_{½}$ and ΔG_o were also significantly lowered ($p < 0.05$) in the presence of eriochrome cyanine R compared to control values. That is, the mechanosensitivity of MscL was greatly increased in the presence of eriochrome.

Based on our study, it is possible that eriochrome cyanine R could be used as a lead compound for the development of a novel type of antibiotic. An antibiotic which would act by gating the mechanosensitive (MS) channels resulting in the leakage of essential ions and cell osmoticants out of the bacterium and thus, prevent its growth and survival.

Bass, R. B., Strop, P., Barclay, M. & Rees, D. C. (2002) *Science* **298,** 1582-1587.

Berrier, C., Coulombe, A., Szabo, I., Zoratti, M. & Ghazi, A. (1992) *European Journal of Biochemistry* **206,** 559-565.

Chang, G., Spencer, R.H., Lee, A.T., Barclay, M.T. & Rees, D.C. (1998) *Science* **282,** 2220-2226.

Levina, N., Totemeyer, S., Stokes, N.R., Louis, P., Jones, M.A. & Booth, I.R. (1999) *EMBO Journal* **18,** 1730-1737.

Martinac, B., Buechner, M., Delcour, A.H., Adler, J. & Kung, C. (1987) *Proceedings of the National Academy Science USA* **84,** 2297-2301.

Nguyen, T., Clare, B., Guo, W. & Martinac, B. (2005) *European Biophysics Journal* in press.

Sukharev, S.I., Blount, P., Martinac, B., Blattner, F. R. & Kung, C. (1994) *Nature* **368,** 265-268.

Sukharev, S. I., Blount, P., Martinac, B. & Kung, C. (1997) *Annual Review of Physiology* **59,** 633-657.

Sukharev, S.I., Martinac, B., Arshavsky, V.Y. & Kung, C. (1993) *Biophysical Journal* **65,** 177-183.

Supported by NH&MRC and a UWA Postgraduate Award to T.N.M. Nguyen.

Mutations within the selectivity filter of the NMDA receptor channel influence voltage-dependent block by extracellular 5-hydroxytryptamine

Anna Kloda and David Adams, School of Biomedical Sciences, University of Queensland, Brisbane QLD 4072, Australia.

The NMDA receptor is a tetrameric cation channel which mediates important physiological processes such as long-term potentiation, synaptic plasticity and neurodegeneration *via* conditional Ca^{2+} signalling. The ionic influx through the open channel pore coincides with the presynaptic release of glutamate and postsynaptic membrane depolarization, which relieves voltage-dependent Mg^{2+} block. The asparagine residue on the NR2 subunit corresponding to position 596 (N+1 site) contributes to the Mg^{2+} binding site and affects channel rectification due to block by extracellular Mg^{2+}. In contrast, asparagine at position 598 (N0 site) on the adjacent NR1 subunits barely affects such events (Wollmuth *et al.*, 1998). Both residues are located near the tip of the M2 re-entrant loop and line the selectivity filter of the channel pore. Recently we reported voltage-dependent inhibition of NMDA receptor currents by 5-hydroxytryptamine (5-HT) (Kloda & Adams, 2005). The voltage sensitivity of the block indicated that 5-HT, similar to Mg^{2+}, binds within the membrane electric field.

In the present study, we assessed the effects of NR1(N0S) and NR2A(N+1Q) mutations of NMDA receptors expressed in *Xenopus* oocytes on the block by extracellular 5-HT using the two-electrode voltage clamp recording technique The mutation within the NR1 subunit of the NR1(N0S)-NR2A receptor combination, strongly reduced the magnitude of the block by 0.3 mM 5-HT and abolished the voltage dependence of block. The corresponding mutation within the NR2 subunit of the NR1-NR2A(N+1Q) receptor channels reduced the block by 5-HT to a lesser extent although the rectification of the I-V curve was similar to that observed for the wild type. This is opposite to the block produced by external Mg^{2+} where a substitution of the NR2A(N+1) site asparagine but not the NR1 N-site significantly reduces the block (Wollmuth *et al.*, 1998). Furthermore, the NR1 and NR2 mutant channels differed in their sensitivities to the 5-HT block compared to wild type. The IC_{50} values for 5-HT block at -120 mV were 59 µM for wild type but increased to 230 µM and 1.5 mM for the NR1 and NR2A mutants, respectively. These data indicate that the block by 5-HT is attenuated by corresponding asparagine mutations in the NR1 and NR2 subunits. The effect of the asparagine substitution in the NR1 and NR2 subunits on 5-HT block suggests that, in contrast to the Mg^{2+} block, 5-HT block critically depends on the NR1 asparagine residue and to a lesser extends on the NR2 residue. Thus, the binding of 5-HT to key residues in a narrow constriction of the channel pore may provide a significant barrier to ionic fluxes through the channel.

Kloda, A. & Adams, D.J. (2005) *British Journal of Pharmacology* 144, 323-330.
Wollmuth, L.P., Kuner, T., & Sakmann, B. (1998) *Journal of Physiology* 506, 13-52.

Ion selectivity of glycine receptors with mutations of charged residues in the intracellular portals

T.M. Lewis[1], Sugiharto[1], J.A. Peters[2], J.J. Lambert[2], P.H. Barry[1] and A.J. Moorhouse[1], [1]School of Medical Sciences, The University of New South Wales, NSW 2052, Australia and [2]Department of Pharmacology and Neuroscience, The University of Dundee, Dundee DD1 9SY, United Kingdom.

The glycine receptor (GlyR) is a member of the nicotinic-like family of ligand gated ion channels that are comprised of five subunits, each with a similar topology of a large N-terminal extracellular domain and four transmembrane domains (TM1 to TM4). The prototypical member of this family is the muscle endplate nicotinic acetylcholine receptor (nAChR). Cryo-electron microscopy studies of nAChRs from the Torpedo electric ray provide the best structural information of this receptor (Unwin, 2005) and by homology, a good template for other members of the family, including the GlyR. The nAChR structure shows that the intracellular loop between TM3 and TM4 is, in part, an α helix (designated 'MA') and the MA helix from each subunit comes together to form an inverted 'tee-pee' underneath the intracellular mouth of the ion channel pore. Charged residues in the MA helix are hypothesized to influence the ion size and charge selectivity of the channel as a consequence of lining the 'portals' or windows that form between adjacent MA helices. In the serotonin receptor (5-HT_3R), these residues influence the channel conductance (Kelley *et al.*, 2003). We investigated homologous residues in the MA helix of the α1 GlyR to see if they influenced ion selectivity or conductance.

Homology alignment of the amino acid sequence for the α1 GlyR subunit and the α subunits of the Torpedo nAChR and 5-HT_3R was used to identify the likely charged residues in the GlyR that line the MA helix and face the portals. Four positively charged residues were identified: Arg377, Lys378, Lys 385 and Lys386. Two mutant α1 GlyR subunits were created: one where all four of these residues were substituted for neutral alanine ('4A') and another where they were substituted for the negatively charged glutamate ('4E'). The cDNA for the wild-type, 4A and 4E GlyR mutants were separately transfected into 293 cells using a polyethylenimine reagent (jetPEI™) and glycine activated currents were recorded using standard whole-cell patch-clamp techniques. Current-voltage (I-V) curves were determined from a voltage-step protocol (100 ms steps) performed during the continued application of non-desensitizing concentration of glycine. I-V curves were initially determined in an extracellular solution containing (in mM): NaCl, 145; glucose, 10; HEPES, 10 (adjusted to pH 7.4). I-V curves were subsequently determined in solutions with 50% NaCl (75 mM) and 25% NaCl (37.5 mM) that were osmotically balanced with sucrose. The internal (pipette) solution was (in mM): NaCl, 145; $CaCl_2$, 2; EGTA, 5; HEPES 10 (adjusted to pH 7.4). The reversal potentials (V_{rev}) were determined from the I-V curves for each NaCl dilution and corrected for liquid junction potentials. The shifts in V_{rev} for each dilution were fitted with the Goldman-Hodgkin-Katz equation to estimate the relative permeability for chloride ions with respect to sodium ions (P_{Cl}/P_{Na}). The mean values for the V_{rev} obtained from the wild-type, 4A and 4E (n=7 in each case) are shown in the following table:

	V_{rev} (mV)		
	wild-type	4A	4E
100% NaCl	-0.3±0.2	-0.3±0.6	-0.8±0.3
50% NaCl	11.6±0.7	10.7±0.5	11.5±0.7
25% NaCl	22.6±1.5	22.4±1.3	22.8±1.4

The corresponding P_{Cl}/P_{Na} values determined were similar in all three cases: 7.5±0.2 for the wild-type, 7.0±0.5 for 4A, and 7.6±0.3 for 4E. These results indicate that the substitution of the four charged residues in the MA helix had no significant effect upon the ion selectivity of the α1 GlyR. Preliminary data suggest that both the 4A and 4E mutations reduce the single channel conductance. Further studies are required to address the possibility that other charged residues lining the portals may be involved in ion selectivity.

Unwin, N. (2005) *Journal of Molecular Biology* **346**, 967-989.
Kelley S.P., Dunlop J.I, Kirkness E.F., Lambert J.J. & Peters J.A. (2003) *Nature* **424**, 321-324.

A molecular determinant of tropisetron inhibition of the glycine receptor Cl^- channel

Z. Yang, A.D. Ney and J.W. Lynch, School of Biomedical Sciences, University of QLD, Brisbane QLD 4072, Australia.

Tropisetron, an antagonist of the 5-HT3 receptor cation channel, is used clinically as an anti-emetic drug. It also has potent effects on the structurally related glycine receptor Cl^- channel (GlyR). At low (sub-micromolar) concentrations, tropisetron potentiates the GlyR and at higher concentrations it produces inhibition (Supplisson & Chesnoy-Marchais, 2000). Since prostaglandins increase the transmission of pain impulses to the brain *via* downregulation of spinal glycinergic neurotransmission, the GlyR has emerged as a novel target for therapies directed at neuropathic pain (Harvey *et al.*, 2004). As a potentiating agent, tropisetron is a lead compound for the development of novel analgesic therapeutics directed at the GlyR. However, the locations of the inhibitory and potentiating tropisetron binding sites on the GlyR are unknown. This study sought to identify the tropisetron inhibitory binding site on homomeric α1 and heteromeric α1β GlyRs.

HEK293 cells were transfected with WT and mutant GlyR cDNA using the calcium phosphate precipitation protocol. When co-transfecting α1 and β subunits, their respective cDNAs were combined in a ratio of 1:10. The transfection solution was removed after 24h and glycine-gated currents were recorded using whole-cell patch clamp techniques over the following 24-72 h. Heteromeric GlyRs were identified by GFP fluorescence coupled to β subunit expression and by their reduced sensitivity of heteromeric GlyRs to picrotoxin.

We first confirmed that sub-micromolar concentrations of tropisetron elicited potentiation and that concentrations above 100 μM inhibited the WT α1 GlyR (Figure, left panel). We then used 500 μM tropisetron to screen a large number of mutant GlyRs in which various known ligand binding sites were abolished. We investigated the principal ligand-binding domain A (*via* mutations I93A, A101H/C, N102A/C/D/Q), domain B (F159A, Y161C) and domain C (K200A, H201A, Y202F, N203A). We also serially eliminated the zinc binding sites (H107N, H109N) and the alcohol binding site (S267C). The four N102 mutations were the only tested mutations that abolished inhibition and in each case this was achieved without affecting tropisetron potentiation (Figure, right panel). When the N102Q mutant α1 subunit was co-expressed with the WT β subunit, tropisetron inhibition returned to near normal potency. N125 in the β subunit residue corresponds to N102 in the α1 subunit. When the N102Q mutant α1 subunit was co-expressed with the N125D mutant β subunit, tropisetron inhibition was also normal.

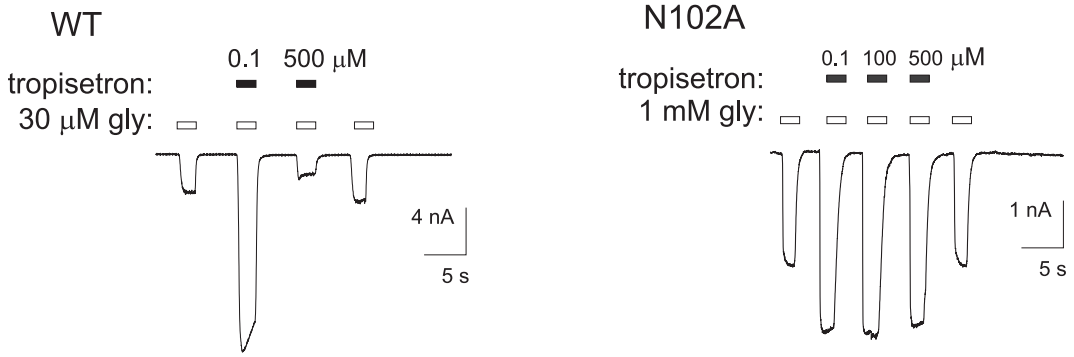

We conclude that N102 in the α1 subunit is a specific determinant of tropisetron inhibition. Its location in the agonist binding pocket implies that it may be a tropisetron binding site. Our results indicate that β subunits also contain tropisetron inhibitory sites. However, the location of the β subunit site does not correspond to its location in the α1 subunit.

Supplisson, S. & Chesnoy-Marchais, D. (2000) *Molecular Pharmacology*, 58, 763-777.

Harvey, R.J., Depner, U.B., Wassle, H., Ahmadi, S., Heindl, C., Reinold, H., Smart, T.G., Harvey, K., Schutz, B., Abo-Salem, O.M., Zimmer, A., Poisbeau, P., Welzl, H., Wolfer, D.P., Betz, H., Zeilhofer, H.U. & Muller, U. (2004) *Science*, 304, 884-887.

Subunit-specific inhibition of recombinantly expressed glycine receptors by ginkgolides and bilobalide

R.L. Hawthorne and J.W. Lynch, School of Biomedical Sciences, University of Queensland, Brisbane QLD 4072, Australia.

Extracts from the ginkgo biloba tree have been used in traditional Chinese medicine for centuries. Major active components of these extracts include the ginkgolides A, B and C (GA, GB, GC) and bilobalide (BB). GA, GB and GC are terpene trilactones which differ only in the number and placement of their hydroxyl groups. They share some structural similarity with BB and with the known glycine receptor Cl^- channel (GlyR) inhibitor, picrotoxin. The ginkgo compounds have recently been shown to have potent inhibitory effects on GlyRs endogenously expressed in cultured central neurons (Kondratskaya *et al.*, 2001; Ivic *et al.*, 2003). Their use- and voltage-dependence suggest they may be pore-blockers (Kondratskaya *et al.*, 2001; Ivic *et al.*, 2003). The aim of the present study was to investigate the specificity of these compounds for recombinantly expressed α1, α2, α1β and α2β GlyRs. Their use-dependence, voltage-dependence and agonist concentration dependence of inhibition were also examined.

HEK293 cells were transfected with GlyR cDNAs by the calcium phosphate precipitation protocol. The α and β subunits were co-expressed in a 1:10 ratio. The transfection solution was removed after 24 h and glycine-gated currents were recorded by whole-cell recording over the following 24−72 h. Heteromeric GlyRs were identified by GFP fluorescence and by their reduced sensitivity to picrotoxin inhibition.

In homomeric α2 GlyRs, inhibition by GA, GB and GC was more pronounced at positive voltages whilst BB showed no significant voltage-dependence. Lower concentrations of glycine markedly increased the inhibitory potency of BB, whereas glycine concentration changes had no significant effect on the degree of inhibition by GA, GB and GC. All four extracts showed use- dependence with no inhibition observed in the absence of glycine. As with picrotoxin, the potency of BB inhibition was drastically reduced upon co-expression of the β subunit with either the α1 or α2 subunits. On the contrary, co-expression of the β subunit with either the α1 or α2 subunits caused a significantly increased sensitivity to GB and GC. The sensitivity to GA was significantly increased in the α2β relative to the α2 GlyR, but was not significantly changed in the α1β relative to the α1 GlyR. The α1 subunit mutation T6′F abolished inhibition by all compounds.

The use-dependence, voltage-dependence and the sensitivity to the pore-lining T6′F mutation, all suggest that the 4 tested ginkgo biloba extracts bind at a site in the GlyR pore. The results however indicate a different mechanism of inhibition by BB compared to that of GA, GB and GC. BB inhibition of the GlyR appears to mimic the effects of picrotoxin, despite these compounds sharing little structural similarity. The subunit-specificity of these compounds may be of use in defining the subunit composition of native neuronal GlyRs. Further investigations are required to examine the molecular basis of the observed differences in their mechanisms and subunit-specificity of action.

Kondratskaya, E.L., Lishko, P.V., Chatterjee S.S. & Krishtal, O.A. (2002) *Neurochemistry International* **40**, 647-653.

Ivic L., Sands, T.T., Fishkin, N., Nakanishi, K., Kriegstein, A.R. & Stromgaard, K. (2003) *Journal of Biological Chemistry* **278**, 49279-49285.

Crosslinking of α1β1 $GABA_A$ receptor subunits *via* cysteines introduced into the transmembrane domain

T.I. Webb, Z. Yang and J.W. Lynch, School of Biomedical Sciences, University of QLD, Brisbane QLD 4027, Australia.

$GABA_A$ receptors belong to the ligand gated ion channel superfamily. Activation of these channels is thought to involve movement of the pore lining M2 domain. A model for α1β1 $GABA_A$ receptor activation has been proposed on the basis of disulphide bond trapping experiments at an M2 residue (T6′) located near the activation gate (Horenstein *et al.*, 2001). This residue was mutated in both subunits to produce αT6′C and βT6′C subunits. Western analysis of $GABA_A$ receptors expressed in HEK293 cells plus electrophysiology of the same receptors in *Xenopus* oocytes suggested that disulphide bonds between adjacent β subunits lock the channels in the open state. The authors conclude that activation is mediated by an asymmetric rotation of adjacent β subunits. Data from our laboratory presented previously (Shan *et al.*, 2002) and here question this model.

To facilitate Western analysis, all αT6′C subunits were tagged with a FLAG epitope and all βT6′C subunits were tagged with a myc epitope. HEK293 cells were transfected with different combinations of wild type α, wild type β, αT6′C and βT6′C subunits and investigated by whole-cell electrophysiological recording. The oxidising agent, copper phenanthroline (Cu:phen), was used to promote formation of disulphide bonds and the reducing agent, dithiothreitol (DTT), was used to break them. Crude membrane preparations of the same transfected subunit combinations were used for Western analyses. Surface expression of functional receptors was confirmed by immunocytochemistry.

Disulphide bond formation between βT6′C subunits was observed in the closed state. In cells expressing channels containing βT6′C subunits, GABA-gated currents decreased irreversibly upon Cu:phen treatment. As this effect was reversed only upon DTT application, we conclude that the disulphide bonds lock the channel closed. These bonds also formed spontaneously at a much slower rate. Western analysis provided direct evidence that formation of disulphide bonds in the closed state occurs between β subunits. The inclusion of DTT at several stages of channel protein preparation was sufficient to reduce the inter-subunit disulphides. Similarly, when Cu:phen was applied in combination with GABA, cells expressing channels containing βT6′C subunits again drastically reduced GABA current magnitude. Since the channels could only be reopened upon a subsequent application of DTT, we conclude that disulphide bonds lock the channel in a closed conformation. Since channels containing βT6′C subunits desensitize rapidly relative to wild type channels, the conclusion that the βT6′C subunits are crosslinked in the open state (simply because GABA is present) should be treated with caution. Due to the very short lifetime of the open state, we suggest that disulphide bond formation occurs predominantly in the desensitized state. Western analysis again provided direct evidence that formation of disulphide bonds in the desensitized state occurs between β subunits. No inter-subunit disulphides were observed with channels containing only αT6′C subunits and β wild type subunits. Indeed, αT6′C subunits were observed to form DTT-sensitive intramolecular disulphides. However, a weak band corresponding to a small population of mixed disulphides was observed with channels containing both αT6′C subunits and βT6′C subunits.

Because we find no evidence for a state-dependent disulphide trapping of T6′C residues, our results are inconsistent with the model for LGIC activation proposed by Horenstein *et al.* (2001).

Horenstein, J., Wagner, D.A., Czajkowski, C. & Akabas, M.H. (2001) *Nature Neuroscience*, **4**, 477-485.
Shan, Q., Haddrill, J.L. & Lynch, J.W. (2002) *Journal of Biological Chemistry*, 277, 44845-44853.

Etomidate alters the single-channel properties of $GABA_A$ receptors in newborn rat hippocampal neurons

V.A.L. Seymour, P.W. Gage and M.L. Tierney, The John Curtin School of Medical Research, The Australian National University, Canberra, ACT 2601, Australia.

The $GABA_A$ receptor is a GABA activated chloride channel that belongs to the superfamily of cysteine-loop ligand-gated ion channels. The receptor is largely responsible for fast inhibitory neural transmission in the mammalian brain and is the target of many drugs including barbiturates, benzodiazepines and general anaesthetics such as etomidate. Etomidate is a carboxylated imidazole general anaesthetic. It is used as an induction agent in rapid sequence intubation in the emergency department because of its fast activation and hemodynamic stability (Bergen & Smith, 1997; Smith *et al.*, 2000).

Whole cell data has shown that etomidate modulates the $GABA_A$ receptor in a number of ways; at clinical concentrations (1-10μM) etomidate potentiates the $GABA_A$ receptor's response to GABA; at higher concentrations (10-1000μM) etomidate can directly activate and desensitize the receptor; and at even higher concentrations (>1000μM) it produces an inhibitory affect (Zhang *et al.*, 2002).

To investigate how etomidate affects the properties of single $GABA_A$ receptors single-channel currents activated by GABA and etomidate are being recorded from hippocampal pyramidal neurons. Neurons are cultured from newborn Wistar rats (<24hours old) and experiments performed from seven days after culture.

Preliminary results indicate that at clinical concentrations (1-10μM) etomidate potentiates the GABA induced current by increasing channel open time, open probability and channel conductance.

The ability of the general anaesthetic etomidate to increase the maximum channel conductance to >40pS adds to our growing list of drugs that are capable of affecting the conductance of $GABA_A$ receptors. Together with diazepam, pentobarbitone, propofol and now etomidate, which may all increase the maximum conductance of $GABA_A$ channels, our data suggest that such drugs are acting through a common molecular mechanism inherent in $GABA_A$ receptors.

Bergen, J.M. & Smith, D.C. (1997) *Journal of Emergency Medicine* **15,** 221-230.
Smith, D.C., Bergen, J.M., Smithline, H. & Kirschner, R. (2000) *Journal of Emergency Medicine* **18,** 13-16.
Zhang, Z.X., Lu, H., Dong, X.P., Liu, J. & Xu, T.L. (2002) *Brain Research* **953,** 93-100.

$GABA_A$ αβ receptors open spontaneously when the conserved M2 leucine 9′ residue is mutated to a threonine

T.L. Luu, M.L. Tierney and P.W. Gage, Division of Molecular Bioscience, The John Curtin School of Medical Research, The Australian National University, ACT 2601, Australia.

Inhibitory neurotransmission in the central nervous system of the brain is largely mediated by the γ-aminobutyric acid type A ($GABA_A$) receptor. This pentameric receptor is selectively permeable to chloride ions when activated by agonist. The simplest functional $GABA_A$ receptor is composed of α and β subunits. Each subunit has 4 transmembrane α-helices, of which the second transmembrane helix (M2) from all 5 subunits forms the pore. At the 9′ position of the M2 is a leucine residue that is conserved in all ligand-gated ion channels.

A single-channel study was performed to examine the effect of substituting the conserved leucine 9′ residue (L9′) to a threonine in the M2 domain in $GABA_A$ αβ receptors. Site-directed mutagenesis was performed on the human α1 and β1 subunit cDNAs. L929 mouse fibroblasts were transfected with either wild type or mutant $GABA_A$ α and β subunits and green fluorescent protein (GFP) plasmids. Successfully transfected cells showed bright green fluorescence and were targeted for single-channel outside-out patch-clamp recordings.

Wild type $GABA_A$ αβ receptors showed single-channel activity when activated by agonist. By contrast, αβ receptors that contained the L9′T substitution in either the α, β or both subunits had spontaneous channel activity. The single-channel activity recorded from wild type αβ receptors in the presence of 1 μM GABA consisted predominantly of brief open time events with a main single-channel conductance of 15 pS. Single-channel activity was recorded from mutant α(L9′T)β and αβ(L9′T) receptors in the absence of agonist. The spontaneous single-channel activity from these two mutant combinations had significantly longer open time events compared to wild type channels, and there was no change in the single-channel conductance. Application of GABA to the mutant α(L9′T)β and αβ(L9′T) receptors led to an increase in single-channel activity. In contrast to the behaviour of α(L9′T)β and αβ(L9′T) receptors, outside-out recordings from the mutant α(L9′T)β(L9′T) receptor showed only a spontaneous leak current with no single-channel closures. The application of penicillin to this spontaneous leak induced very brief closures.

The data suggest that in wild type αβ receptors the functional role of the L9′ residue is to stabilise the closed state of the channel. When mutated to a threonine the equilibrium of the receptor is pushed towards the open state as revealed by the ability of mutant receptors to now open spontaneously.

GABARAP influences the conductance of recombinant $GABA_A$ channels

A.B. Everitt, M.L. Tierney and P.W. Gage, The John Curtin School of Medical Research, Australian National University, Canberra, ACT, Australia.

'Native' $GABA_A$ receptors display distinct electrophysiological properties not always seen in recombinant receptors irrespective of subunit composition. Native channels can have conductances over 40pS (Gray & Johnson, 1985; Smith *et al.*, 1989: Curmi *et al.*, 1993). Moreover, the conductance of some channels can be increased by modulating drugs such as diazepam, pentobarbitone and propofol (Eghbali *et al.*, 1997; Guyon *et al.*, 1999; Eghbali *et al.*, 2003). By contrast, conductances of recombinant channels have never exceeded 35pS and, although their open probability can be increased by modulating drugs, channel conductance was not enhanced by drugs.

A $GABA_A$ receptor-associated protein, GABARAP, is an intracellular protein that can interact with the $GABA_A$ γ2 subunit. When co-expressed with $GABA_A$ subunits, GABARAP caused clustering of the receptors and changes in whole-cell current kinetics in QT6 fibroblasts (Wang *et al.*, 1999). Recent observations have shown that over-expression of GABARAP in *Xenopus* oocytes and in neurons increases the level of $GABA_A$ receptors detected at the plasma membrane, indicating that GABARAP is involved in the trafficking of $GABA_A$ receptors (Chen *et al.*, 2005; Leil *et al.*, 2004).

It has been suggested that high channel conductances may represent co-operative openings of clustered channels resulting in an apparent high single channel conductance (Laver & Gage, 1997). We tested this hypothesis in an expression system by co-expressing GABARAP, known to cluster $GABA_A$ receptors, with $GABA_A$ receptor subunits in L929 mouse fibroblasts.

Immunofluorescent studies revealed that co-expression of GABARAP with $GABA_A$ subunits, showed a punctate pattern of staining of surface receptors compared to a diffuse pattern in control cells.

We recorded single channel currents in the cell-attached (c/a) configuration 24-72 hours post transfection. Control patches expressing $GABA_A$ α1, β1 and γ2s subunits alone had a mean conductance of 22.3 ± 1.2 pS (n=15). In 16 out of 25 patches recorded from cells co-transfected with $GABA_A$ α1, β1 and γ2s subunits and GABARAP, single channel conductances were above 40pS (γ = 60.7 ± 4.3pS, n=16). These 'high' conductance channels were never seen in control patches. In the remaining 9 patches, the mean conductance was 29.1 ± 1.9 pS. Both high and low conductance channel activities were blocked by 100μM bicuculline. The current-voltage relationship of high conductance channels showed outward rectification of the current, similar to that seen in native receptors.

Diazepam and pentobarbital have been shown to increase both open probability and conductance of $GABA_A$ channels. In patches from cells co-expressing $GABA_A$ α1, β1 and γ2s subunits and GABARAP, both of these effects were seen irrespective of initial channel conductance. In control patches where GABARAP was not expressed, application of diazepam or pentobarbital increased the channel open probability with no effect on single channel conductance.

Our results show that co-expression with GABARAP has changed the properties of recombinant $GABA_A$ channels. It is possible that clustered receptors may be able to couple and open cooperatively by virtue of their close physical proximity.

Curmi, J.P., Premkumar, L.S., Birnir, B. & Gage, P.W. (1993), *Journal of Membrane Biology*, 136, 273-280.
Eghbali, M., Curmi, J.P., Birnir, B. & Gage, P.W. (1997), *Nature*, 388, 71-75.
Eghbali, M., Gage, P.W. & Birnir, B. (2003), *European Journal of Pharmacology*, 468 (2): 75-82.
Gray, R., Johnston, D. (1985) *Journal of Neurophysiology*, 54: 134-142.
Guyon, A., Laurent, S., Paupardin-Tritsch, D., Rossier, J. & Eugen, D. (1999), *Journal of Physiology*, 516, 719-737.
Smith, S.M., Zorec, R. & McBurney, R.N. (1989) *Journal of Membrane Biology*, 108, 45-52.
Wang, H., Bedford, F.K., Brandon, N.J., Moss, S.J. & Olsen, R.W. (1999), *Nature*, 397, 69-72.
Chen, Z., Chang-Sheung, S., Leil, T.A., Olcese, R. & Olsen, R.W. (2005), *Molecular Pharmacology*, 68(1), 152-159.
Leil, T.A., Chen, Z., Chang-Sheung, S. & Olsen, R.W. (2004), *Journal of Neuroscience*, 24(50): 11429-11438.
Laver, D.R.. & Gage, P.W. (1997), *Prog. Biophsy. Mol. Biol*, 67: 99-140.

C-Terminal peptide of M protein from dengue virus (DVM-C) forms ion channels

A. Premkumar, C.R. Horan and P.W. Gage, Division of Molecular Biosciences, John Curtin School of Medical Research, Australian National University, PO Box 334, Canberra City, ACT 2601, Australia.

The dengue virus belongs to the family of Flaviviridae and causes an infectious disease carried by mosquitoes - dengue fever. There is no specific treatment for dengue fever, and most people recover completely within 2 weeks.

Like the alphaviruses and influenza viruses, the dengue virus enters cells in an endocytotic vesicle. The M, or membrane protein, of the dengue virus may have a similar function to that of the M2 protein of Influenza A and assist in the entry of the virus by functioning as an ion channel. The M protein is one of the structural proteins of the virus and is 75 amino acids in length. The C-terminal end of the protein from amino acids 48 to 70 contains a predicted transmembrane region, thought to anchor the protein in the lipid bilayer (Kuhn *et al.*, 2002). The function of the M protein is still unknown. To test the hypothesis that the M protein of dengue functions in a similar manner to the M2 protein of influenza A we tested the C-terminal end of the M protein containing the putative transmembrane region for channel activity.

The C-terminus of the M protein of the Dengue virus type 1 strain Singapore S275/90 (DVM-C) was chemically synthesised and tested for channel forming properties in artificial lipid bilayers.

We have found that the DVM-C peptide from Dengue virus forms ion channels in lipid bilayer membranes. The channels were selective for monovalent cations over monovalent anions but were relatively impermeable to calcium ions. Amantadine (10 μM) and 100 μM Hexamethylene amiloride (HMA) block channels formed by DVM-C. The dengue virus M protein can be added to an increasing list of virus proteins that have been shown to form ion channels in artificial lipid bilayers.

Kuhn, R.J., Zhang, W., Rossmann, M.G., Pletnev, S.V., Corver, J., Lenches, E., Jones, C.T., Mukhopadhyay, S., Chipman, P.R., Strauss, E.G., Baker, T.S., Strauss & J.H. 2002. *Cell* 108**:**717-25.

The role of the M1-P1 loop in acid sensitive two-pore domain potassium (TASK) channel regulation

Catherine E. Clarke[1,2], Alistair Mathie[3] and Jamie I. Vandenberg[1,2], [1]St Vincent's Hospital Clinical School, University of New South Wales, Victoria Road, Darlinghurst NSW 2010, Australia, [2]Electrophysiology and Biophysics Unit, Victor Chang Cardiac Research Institute, 384 Victoria Street, Darlinghurst, NSW 2010, Australia and [3]Department of Biological Sciences, Imperial College London, Exhibition Road, London SW7 2AZ, UK.

Background potassium channels control the resting membrane potential of many cells and regulate their excitability. Two-pore-domain potassium (2PK) channels have been shown to underlie a number of such background currents. Although often classed as "leak" channels, currents through 2PK channels are tightly regulated. For example, the acid sensitive 2PK (TASK) channels are inhibited by extracellular acidification with pKa's for TASK-1, TASK-2 and TASK-3 ranging from 6.5 to 8.5. TASK channels show relatively high homology in their transmembrane domains, but very little homology in extracellular domains, most notably in the ~50 residue linker between the first transmembrane domain and the first pore domain (the M1P1 loop). The M1P1 loop has previously been shown to be involved in the differential sensitivity of TASK channels to block by zinc (Clarke *et al.*, 2004). The aim of the present study was to test the hypothesis that the M1P1 loop contributes to the differential pH sensitivity of TASK channels. Chimaeric TASK channels were constructed by swapping M1P1 loops between family members and expressed in Chinese Hamster Ovary cells. Channels were characterised using standard whole cell patch clamp techniques. The chimaera formed from TASK-3 with the TASK-1 M1-P1 loop (T3/T1-M1P1) had a pK_a for inhibition that was much more similar to that of TASK-1 than TASK-3 (T1/T3 M1P1: $pK_a = 7.0 \pm 0.05$, TASK-1: $pK_a = 7.1 \pm 0.04$; TASK-3, $pK_a = 6.7 \pm 0.07$). This indicates that the M1P1 loop contributes to the differential pH sensitivity of TASK-1 and TASK-3 channels. All other chimaeras, however, were non-functional. This further suggests that the M1P1 loops are important for function and/or structure. However, further work needs to be done to assess whether these non-functional chimaeras are reaching the membrane and whether function can be restored through re-addition of further regions of the channel, such as the P-loop.

Clarke, C.E., Veale, E.L., Green, P.J., Meadows, H.J. & Mathie, A. (2004) *Journal of Physiology* **560**, 51-62.

Structural studies of chloride intracellular ion channel proteins

A.V. Mynott[1], D.R. Littler[1], P.M.G. Curmi[1], L.J. Brown[2] and S.N. Breit[3], [1]School of Physics, University of New South Wales, NSW 2052, Australia, [2]Department of Chemistry and Biomolecular Sciences, Macquarie University, NSW 2109, Australia and [3]St Vincent's Hospital, Sydney, NSW 2010, Australia.

The chloride intracellular channel (CLIC) family of proteins belong to a new class of chloride ion channels. They are generally localised on the nuclear membrane, but are also found in the cytoplasm and on the cell membrane. They have the unique feature of existing in both soluble and membrane associated forms.

The structural conformation of these proteins may be affected by various biological mechanisms including pH, redox and interactions with binding partners. For example, suggestions of CLIC translocation to the nucleus under stress has led to speculation of a direct interaction of CLIC with components of the nuclear import machinery. Furthermore, the location of the conserved cysteine residues in the 3-dimensional structure of the CLIC proteins may also prove crucial to the understanding of the structure-function relationship.

In this study, members of the CLIC family have been examined using various biophysical techniques, including circular dichroism spectroscopy, to reveal possible structural conformational changes that may occur under variations in environmental conditions. The conditions examined include binding partner interactions, oxidation and mutagenesis of the conserved cysteine residues. Results suggest that changes in these conditions, particularly mutation of Cys178 in CLIC1, lead to conformational instability and structural differences.

Photochemical behaviour and Na^+,K^+-ATPase sensitivity of voltage-sensitive styrylpyridinium fluorescent membrane probes

S. Amoroso[1], V.V. Agon[1], T. Starke-Peterkovic[1], M.D. McLeod[1], H.-J. Apell[2], P. Sebban[3] and R.J. Clarke[1], [1]School of Chemistry, University of Sydney, NSW 2006, Australia, [2]Faculty of Biology, University of Constance, D-78434 Constance, Germany and [3]Laboratory of Physical Chemistry, UMR 8000, University of Paris XI, Orsay 91405, France.

Styrylpyridinium dyes are widely used probes of electric field strength changes in biological membrane systems. They can be used as optical probes in the imaging of electrical activity in nerve and muscle cells, and for the investigation of the mechanisms of electrogenic ion pumps. A limit to their application is, however, their photochemical stability. Probes with improved stability and voltage sensitivity are required in order to extend their areas of application.

Exposure of the voltage-sensitive membrane probe RH421 to continuous illumination with 577 nm light from an Hg lamp leads to an increase in its steady-state fluorescence level when bound to lipid membranes. The increase occurs on the second time-scale at typical light intensities and was found to be due to a single-photon excited-state isomerisation. In order to suppress this undesirable reaction, modifications to the dye structure are, therefore, necessary. The related probe ANNINE 5, which has a rigid polycyclic structure, shows no observable photochemical reaction when bound to DMPC vesicles on irradiation with 436 nm light. The voltage sensitivity of ANNINE 5 was tested using Na^+,K^+-ATPase membrane fragments. As long as ANNINE 5 is excited on the far red edge of its visible absorption band, it shows a similar sensitivity to RH421 in detecting charge-translocating reactions triggered by ATP phosphorylation. Unfortunately, the wavelengths necessary for ANNINE 5 excitation are in a region where the Hg lamps routinely used in stopped-flow apparatus have no significant lines available for excitation.

Applications of styrylpyridinium dyes in elucidating ion-transport mechanisms in plant cells

S. Amoroso[1], R.J. Clarke[2], A. Larkum[1] and R. Quinnell[1], [1]School of Biological Sciences, University of Sydney, NSW 2006, Australia and [2]School of Chemistry, University of Sydney, NSW 2006, Australia.

Styrylpyridinium dyes have been used in a range of biological applications, including quantitative electrophysiology and qualitative microscopy for the detection of the membrane electric field strength changes. Examples of these dyes include RH421 and di-4-ASPBS. The aims of our project are to extend the applications of styrylpyridinium dyes and to elucidate ion-transporting mechanisms that take place within algal systems. The dyes RH421, di-4-ASPBS, Annine V, RH414, RH795 and RH237 have been tested on a freshwater photosynthetic system, *Chara corallina* and preliminary measurements have shown that all of these dyes are successfully taken up by the membranes of *Chara* cells. The potential of these molecules to detect ATPase activity is under examination. In addition, we are examining the ability of these molecules to detect the effects of membrane transport inhibitors and protonophores. So far, we have concluded that the styrylpyridinium dye, di-4-ASPBS is the most useful dye for resolving these processes in a freshwater alga cell. These preliminary results are encouraging, as these particular dyes have not previously been applied in photosynthetic systems.

The crystal structure of *Pichia pastoris* lysyl oxidase at 1.23Å reveals a lysine-lysine covalent cross-link, dehydrolysinonorleucine

A.P. Duff[1], A.E. Cohen[2], P.J. Ellis[2], D.B. Langley[1], D.M. Dooley[3], H.C. Freeman[1] and J.M. Guss[1], [1]School of MMB, University of Sydney, NSW 2006, Australia, [2]Stanford Synchrotron Radiation Laboratory, CA, USA and [3]Chemistry and Biochemistry, Montana State University, Bozeman MT, USA.

We have refined the structure of *Pichia pastoris* lysyl oxidase (PPLO) in a new crystal form at 1.23Å resolution with R = 0.112 and Rfree = 0.146. PPLO is a copper amine oxidase (CuAO) containing a trihydroxyphenylalanine quinone (TPQ) cofactor. PPLO is unusual in being able to oxidise the side chain of lysine residues in a polypeptide. In this respect, it is functionally related to another class of CuAOs of unrelated sequence, which contain the related quinone cofactor, lysine tyrosylquinone (LTQ). The asymmetric unit comprises residues 43 to 779 of the polypeptide, 7 carbohydrate residues, the active-site Cu atom, an imidazole molecule bound in the substrate-binding site, 2 buried Ca^{2+} ions, 5 surface Mg^{2+} ions, 5 surface Cl^{-} ions, and 1045 water molecules. The cofactor, TPQ, and some other active site residues are poorly ordered, in contrast to the high degree of order of their other neighbours. A covalent cross-link between two lysine residues, Lys 778 and Lys 66, is observed. The cross-link, dehydrolysinonorleucine, is formed by the oxidation of Lys 778, followed by spontaneous reaction with Lys 66.

Molecular dynamics study of conformational changes in human serum albumin by binding of fatty acids

S. Fujiwara and T. Amisaki, Department of Biological Regulation, Faculty of Medicine, Tottori University, 86 Nishi-machi, Yonago, 683-8503, Japan.

Human serum albumin (HSA) is a major protein component of blood plasma. Binding of drugs to HSA is one of the most important factors determining pharmacokinetics of drugs (Kragh-Hansen *et al.*, 2002). When measuring binding affinity of a drug to HSA *in vitro*, defatted HSA is usually used. On the other hand, under normal physiological conditions, HSA binds with fatty acid. So far, there is little information on conformational changes of HSA upon binding of fatty acids. The present study was aimed to elucidate the conformational changes as well as the structure and dynamics of HSA, based on the molecular dynamics (MD) simulations with explicit water molecules.

Materials and methods. The initial coordinates of unliganded HSA and HSA-myristate (HSA-MYR) complex were obtained from Protein Data Bank (unliganded HSA: PDB entry 1AO6, HSA-MYR: PDB entry 1BJ5). A series of MD calculations were carried out using AMBER7 package (Case *et al.* 2002). A rectangular-shaped box of water was constructed. 5 ns MD calculations were carried out for both the unliganded HSA and HSA-MYR complex models under periodic boundary condition. The long-range electrostatic interactions were handled by the particle mesh Ewald algorithm (Darden *et al.*, 1993). The resultant model systems contained 87223 (unliganded HSA) and 99126 (HSA-MYR complex) atoms, respectively.

Results and discussion. The root mean square deviation (RMSD) from the X-ray structure over the course of a MD simulation reached plateau at about 2 ns. The RMSD values were as small as about 3.0 Å, which were roughly comparable to the X-ray resolution. Hence, we concluded that significant structural drift from the X-ray structure did not occur during the MD simulations.

Binding of MYR to HSA increased the radius of gyration (Rg) of HSA in the MD simulations. Through the structural comparison of the average structures, the dramatic extent of the relative motions of domains I and III, especially those of subdomains IA and IIIB, were observed. Thus, increase in Rg by binding of MYR molecules should be observed for HSA, as a result of the motions of domains I and III.

Local protein mobility was analyzed by calculating the time-averaged root mean square fluctuation (RMSF) for each residue, using the trajectory in an equilibrium state. RMSF values at drug binding sites I (subdomain IIA) and II (subdomain IIIA) were increased by binding of MYR. This result implies that binding affinity of drugs at these primary binding sites can be changed by MYR binding.

To analyze internal motions of the whole HSA molecule and each domain, principal component analysis for collective coordinates from MD simulations was carried out. The primary internal motions, characterized by the first and the second principal components, PC1 and PC2, were observed mainly at domains I and III. The directional motion projected on PC1 of unliganded HSA was similar with that projected on PC2 of HSA-MYR complex, indicating that the first principal directional motion in unliganded HSA is conserved as the second principal directional motion in HSA-MYR complex. On the other hand, the second principal directional motion in unliganded HSA partially turned into the first principal directional motion in HSA-MYR complex.

Conclusion. The present study unraveled possible conformational changes in aqueous solution caused by binding of MYR molecules to HSA, based on the results of the MD simulations.

Case, D.A., Pearlman, D.A., Caldwell, J.W., Cheatham, T.E. 3rd, Wang, J., Ross, W.S., Simmerling, C.L., Darden, T.A., Merz, K.M., Stanton, R.V., Cheng, A.L., Vincent, J.J., Crowley, M., Tsui, V., Gohlke, H., Radmer, R.J., Duan, Y., Petera, J., Massova, I., Seibel, G.L., Singh, U.C., Weiner, P.K., Kollman, P.A. (2002) AMBER7. San Francisco: University of California.

Darden, T., York, D., Pedersen, L. (1993) *Journal of Chemical Physics* 98, 10089-10092.

Kragh-Hansen, U., Chuang, V.T.G., Otagiri, M. (2002) *Biological and Pharmaceutical Bulletin* 25, 695-704.

NMR probes of red cell deformation

P.W. Kuchel, B.E. Chapman, D.J. Philp and W.A. Bubb, School of Molecular and Microbial Biosciences, University of Sydney, NSW 2006, Australia.

The mean circulation time of a red blood cell (RBC) in an adult human is ~1 minute. Thus each RBC in passing through the peripheral and the pulmonary capillary beds undergoes deformation, from its biconcave-disc shape to an elongated bullet shape, and the reverse, every 30 seconds.

^{23}Na and ^{133}Cs nuclei have spin >1/2 and thus a nuclear electric quadrupole. This renders their NMR resonance frequency sensitive to the presence of electric field gradients at binding surfaces. Such gradients exist in anisotropic media.

Gelatine, which sets at temperatures below ~30°C, was cast inside a silicone rubber tube that in turn was placed inside a glass tube. Thus the gelatine could be stretched by a factor of up to ~2; in the process the gelatine developed structural anisotropy. This anisotropy was evident as a splitting into three of the $^{23}Na^{+}$ NMR resonance, whereas the $^{133}Cs^{+}$ NMR resonance was split into a septet. In both cases the residual quadrupolar coupling constant was a linear function of the extent of stretching.

RBCs set in the gelatine revealed separate resonances for $^{133}Cs^{+}$ inside and outside the cells. And, stretching the gelatine also stretched the RBCs as was apparent from the emergence of quadrupolar splitting of the intracellular $^{133}Cs^{+}$ resonance.

Finally, the metabolic activity of the RBCs was measured using ^{13}C NMR, with D-[U-^{13}C]glucose as substrate, when the cells were in the stretched or unstretched states.

These findings allow comment on the energy cost of the return of an RBC to its equilibrium shape, after distortion.

Current-voltage analysis of response to salt stress by salt-tolerant and salt-sensitive charophyte cells

Mary J. Beilby and Virginia A. Shepherd, Biophysics, School of Physics, University of NSW, NSW 2052, Australia.

The electrophysiological responses of salt-tolerant charophyte *Laprothamnium succinctum* and salt-sensitive charophyte *Chara corallina* to NaCl increase in the medium are compared. The modelling of the current-voltage (I/V) curves allow us to resolve the response of various transporter populations from the total clamp current. The proton ATPase I/V profile is fitted by the HGSS (Hansen, Gradmann, Slayman and Sanders) model of the proton pump (Beilby, 1984). The background current is fitted by an empirical model. The inward K^+ rectifier in *Lamprothamnium* is modelled by the GHK (Goldman, Hodgkin, Katz) model supplemented by the Boltzmann distribution (Beilby & Walker, 1996).

In both charophytes there is a greater background conductance as Na^+ concentration in the medium rises. *Lamprothamnium* is able to maintain the negative resting PD (potential difference) by increasing the rate of proton pumping. The HGSS pump model rate constants k^0_{io}, k^0_{oi} and κ_{oi} all increase over about 120 min of the salt stress (+ 72 mM NaCl). The inward rectifier activates at more positive PDs.

Chara cells, faced with hypertonic medium of 50 mM NaCl and 0.5 mM Ca^{++} added to the APW (artificial pond water), exhibit more varied responses: (i) pump rate was unchanged, (ii) k^0_{io}, k^0_{oi} increased but not κ_{oi}, (iii) k^0_{io}, k^0_{oi} and κ_{oi} all increased over 80 min. However, the pumping increase in *Chara* is not enough to keep the membrane from depolarizing. Further, the proton pump becomes very sensitive to both depolarization and hyperpolarization imposed on the membrane. Pump inhibition follows and the recovery is very slow. This instability of the pump impedes recovery of the negative resting PD after voltage clamp to a bipolar staircase command or a spontaneous action potential. It is also impossible to voltage clamp the membrane to sufficiently negative PD levels to investigate the effect of high salt on the inward rectifier.

Charophytes are evolutionarily most closely allied to the green algal line that gave rise to higher plants (Graham & Gray 2001; Karol *et al.*, 2001) and therefore make good models for them. The significance of the differences in one type of transporter rendering the plant cell salt-tolerant can be considered in the light of evolutionary adaptations.

Beilby M.J. (1984) *Journal of Membrane Biology* **81**, 113-125.
Beilby M.J. & Walker N.A. (1996) *Journal of Membrane Biology* **149**, 89-101.
Graham, L.E. & Gray J. (2001) In: Gensel, P.G. & D. Edwards (eds), Plants Invade the Land. Evolutionary and Environmental Perspectives. Columbia University Press, New York: 140-159.
Karol, K.G., McCourt R.M., Cimino M.T. & Delwiche C.F. (2001) *Science* **294**, 2351-2353.

Oxygen evolution in chimeric spinach photosystem II with cyanobacteria manganese stabilising protein

Adele Williamson, Warwick Hillier, Reza Razeghifard and Tom Wydrzynski, Photobioenergetics Group, Research School of Biological Sciences, The Australian National University, Canberra, ACT 0200, Australia.

Photosystem II (PSII) is the first multiprotein complex in the photosynthetic electron transfer chain and catalyses the light-driven oxidation of water and reduction of plastoquinone. The PSII protein contains a sub domain termed oxygen evolving complex (OEC), where water is split during photosynthesis, and oxygen released as a by product. The OEC is made up of loop regions of the core membrane spanning subunits, a cluster of Mn_4Ca ions which are the site of water oxidation, and three extrinsic proteins which are bound electrostatically to the core proteins. Of these extrinsic proteins, only the 33kDa manganese stabilising protein (MSP) is common to higher plants, algae and cyanobacteria. The MSP is essential for stabilising Mn binding and provides optimal O_2 evolution. However the MSP does not appear to provide any ligands to any of these ions and its function was proposed to facilitate O_2 production by forming a channel which controls entry of the substrate water to the active site or release of the O_2 and proton products (De Las Rivas & Barber, 2004; Ferreira *et al.*, 2004; Wydrzynski *et al.*, 1996).

In this presentation we have created chimeric PSII complexes by removing all three extrinsic proteins from the PSII complex of spinach, and replacing the native MSP with recombinant MSP from the thermophilic cyanobacterium *Thermosynechococcus elongatus.* The recombinant protein is either fused with thioredoxin or truncated by 39 amino acids at the C-terminus resulting in a deletion of the conserved water channel residues. Here we present the O_2 evolution and tyrosine radical decay kinetics of these chimeric proteins. The results show the importance of these conserved residues to catalytic function and suggest that substrate accessibility is important for this enzyme.

De Las Rivas, J. & Barber, J. (2004) *Photosynthesis Research* **81**, 329-343.
Ferreira, K.N., Iverson, T.M., Maghlaoui, K., Barber, J., & Iwata, S. (2004) *Science* **303**, 1831-1838.
Wydrzynski, T., Hillier, W., & Messinger, J. (1996) *Physiologia Plantarum* **96**, 342-350.

The role of an oil droplet lens in vision enhancement

L. Fischer[1], M. Vorobyev[2], A. Zvyagin[1] and T. Plakhotnik[1], [1]Department of Physics, University of Queensland, QLD 4072, Australia and [2]Vision Touch and Hearing Research Centre, University of Queensland, QLD 4072, Australia.

The cone photoreceptors of all birds and some reptiles, amphibians, mammals and fish contain both coloured and transparent oil droplets (Walls, 1942). The light incident on the photosensitive region of such receptors is preconditioned by this oil droplet lens. Coloured oil droplets (which form the majority of the oil droplet population) act as long-pass filters and are thus responsible for spectral tuning. The prevalence of transparent oil droplets throughout the vertebrate classes, such as the T-type oil droplets found in the Ultraviolet or Violet-Sensitive (UVS/VS) photoreceptors of birds, suggests an auxiliary dioptric function operating outside of colour filtering (Young & Martin, 1984). It is hypothesized that an oil droplet lens enhances light collection efficiency and - perhaps more importantly - detection directionality. The outstanding features of an idealised photoreceptor can be modelled in the framework of the electromagnetic theory. The table indicates the set of characteristic parameters that are used in the construction of this model.

Model Parameter	**Value (μm)**
Oil Droplet	2.5
Outer Segment (OS) Length	10.0
OS Base Diameter	1.5
OS Tip Diameter	1.0
Region	**Refractive Index**
Cone Outer Segment	1.387 - 0.0011*i*
Extracellular Matrix	1.340
Transparent Oil Droplet	1.480

The geometric optics approximation cannot be applied to this problem since the wavelength of light and the dimensions of the system are of a comparable order of magnitude. The dioptric function of oil droplets has previously been considered in the context of the Mie scattering theory, which provides an analytic solution to Maxwell's equations of electromagnetics for spherical particles (Ives, Normann & Barber, 1983). Due to the complexity of any realistic photoreceptor structure, a complete analytic solution is not possible. Rather, numerical methods within electromagnetic theory must be employed. The Finite-Difference Time-Domain technique (FDTD) appears to be an attractive alternative to investigate the light coupling efficiency of the photosensitive region in the presence of an oil droplet. FDTD provides a full field solution of Maxwell's equations for some specific dielectric structure. Numerical data sets have been obtained for the vertebrate photoreceptor structures of rods, cones and cones containing transparent oil droplets under broad-band plane wave excitation. Preliminary results show that in the presence of an oil droplet, cones have an increased light coupling efficiency whilst in the retinal mosaic.

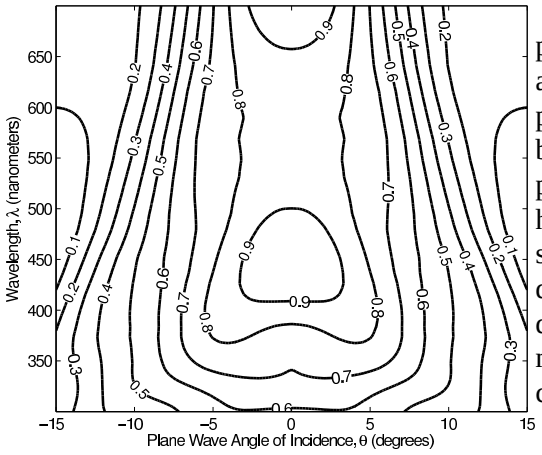

The normalised plane wave coupling efficiency of a cone photoreceptor containing an oil droplet is shown in the figure. It is a function of both the wavelength and the angle of incidence of the plane wave. Maximal coupling at normal incidence is significantly blue-shifted when preconditioned by an oil droplet lens. Since the photopigment found in UVS/VS photoreceptors characteristically have absorption maxima between 360 and 430 nm, such peak shifting is indicative of spectral tuning. Both the geometry and dielectric properties of photoreceptors are expected to change during *in vitro* analysis. Thus, numerical investigation of the model parameters that determine the degree of peak shifting is currently being conducted.

Ives, J.T., Normann, R.A. & Barber, P.W. (1983) *Journal of the Optical Society of America* **73**(12), 1725-1731.

Walls, G.L. ed. (1942) *The vertebrate eye and its adaptive radiation.* Bloomfield Hills, Cranbrook Institute of Science.

Young, S.R. & Martin, G.R. (1984) *Vision Research* **24**(2), 129-137.

Circular dichroic spectra of the N-terminal region of cardiac myosin binding protein – C

C.E. Oakley[1], L.J. Brown[2] and B.D. Hambly[1], [1]Department of Pathology, University of Sydney, NSW 2006, Australia and [2]Department of Chemistry and Biomolecular Sciences, Macquarie University, NSW 2109, Australia.

Myosin binding protein – C (MyBPC) is a multi-domain protein whose role in the sarcomere is complex and not yet fully understood. Three isoforms of human MyBPC have been identified; fast skeletal, slow skeletal and cardiac. The cardiac isoform has been of particular interest because of its link to the heart disease familial hypertrophic cardiomyopathy (FHC). FHC is caused by the expression of abnormal contractile proteins in the heart muscle including numerous mutations in MyBPC. The core structure of cardiac MyBPC consists of eight immunoglobulin (IgI) and three fibronectin (FnIII) domains, numbered 0 – 10 from the N-terminus.

MyBPC is phosphorylated up to 3 times near the N-terminus and this is associated with increased contractile force. The binding of MyBPC to myosin S2 in a phosphorylatable-dependent manner is well established, although the role of the extent of phosphorylation is unknown. The location of phosphorylation is a linker of about 100 amino acids between IgI domains 1 and 2. The focus of this work is the effect of phosphorylation and FHC mutations on the structure of the linker or the IgI domains that flank it.

The N-terminal IgI motifs, C1C2, have been cloned, expressed, purified and circular dichroic (CD) spectra for (i) the wild type, (ii) the “permanently” phosphorylated mutants (Ser to Asp) and (iii) 9 FHC mutants collected. The spectra indicate that a proportion of the protein is alpha-helix. Modelling of the C1C2 construct also suggested an alpha-helical content and indicated that it is likely to be part of the phosphorylation linker region. Changes in the CD spectra of the FHC mutants indicate a change in secondary structure and may explain the pathogenesis of these mutations. Similarly, a change in spectra due to pseudo-phosphorylation may provide an insight into the functional role of MyBPC in the sarcomere.

Changes in mechanical properties of live cell wall during turgor regulation monitored by atomic force microscopy

E.M. Mahomudally[1], M.J. Beilby[2], V. Shepherd[2] and A.R. Moon[1], [1]Department of Applied Physics, University of Technology, Sydney, NSW 2007, Australia and [2]Biophysics Department, School of Physics, University of New South Wales, Kensington, NSW 2052, Australia. (Introduced by M.J. Beilby)

Plant cells display mechanosensitivity (Shepherd *et al.*, 2001). Monitoring these mechanical signals *via* changes in the cell wall is important in the study of control pump activation during hypotonic turgor regulation (Bisson & Beilby, 2002).

The atomic force microscope (AFM) has become a useful tool in the study of surface mechanical properties (Burnham & Colton, 1989). In the study of biological samples its great advantage is allowing real-time study of samples in their native state (Radmacher, 1997). We have used the AFM to monitor changes in mechanical properties of the cell wall as the cell is subject to osmotic stress.

We report on experiments conducted on small live cells (2-3mm) of *Ventricaria ventricosa (Valonia)*, a well characterised, large single-celled alga. Measurements were taken on the resting cell in artificial seawater (ASW 990 mOsmol•kg^{-1}) prior to initiating turgor regulation. Hypotonic stress of 200 mOsmol•kg^{-1} was then imposed on the cell. After stabilisation, measurements were collected on the cell surface for approximately 2 hours. The procedure was repeated for an additional hypotonic shock of 590 mOsmol•kg^{-1}.

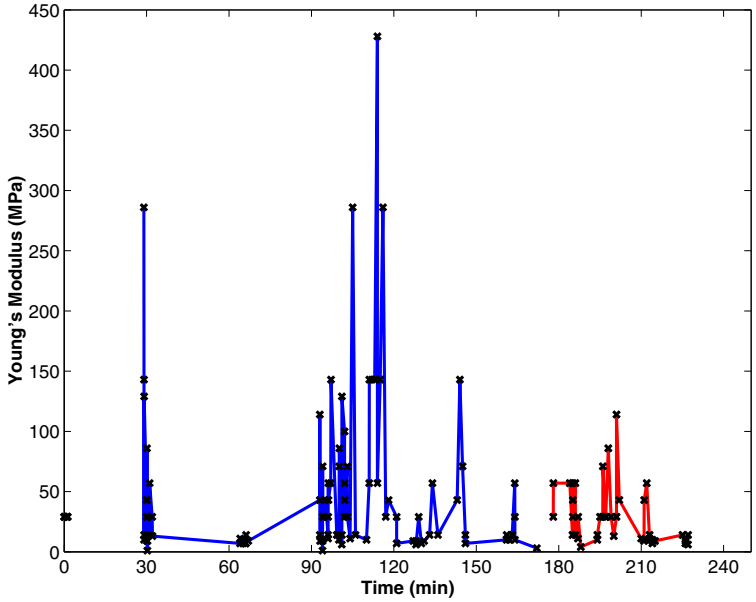

The figure shows the time response of the cell stiffness. The cell appears to respond to hypotonic shock by rapidly altering its wall. Soon after the onset of hypotonic shock, wall strengthening is observed, then a period of large oscillations between wall strengthening and weakening is seen followed by a period of smaller oscillations. A weak wall compared to the resting cell's was observed after the oscillation period. The cells examined survived the two levels of hypotonic shock.

Bisson, M.A. & Beilby, M.J. (2002) *The Journal of Membrane Biology* **190,** 43-56.
Burnham, N.A. & Colton, R.J. (1989) *Journal of Vacuum Science and Technology A* **7**, 2906-2913.
Radmacher, M. (1997) *IEEE Engineering in Medicine and Biology* **16**, 47-57.
Shepherd, V.A., Shimmen, T. & Beilby, M.J. (2001) *Australian Journal of Plant Physiology* **28**, 551-566.

Effect of temperature on stretch-induced cardiac action potential shortening in the rat heart: involvement of TREK-1

D.R. Kelly, L. Mackenzie and D.A. Saint, Discipline of Physiology, School of Molecular and Biomedical Science, University of Adelaide, SA 5005, Australia.

The importance of stretch activated ion channels in the modulation of cardiac electrophysiology is becoming increasingly apparent. Of the stretch activated channels known, both temperature sensitive TREK-1 and non-selective cation channels exist in the rat heart. The present study aimed to evaluate the contribution of these stretch-activated channels to changes in the rat cardiac action potential duration during stretch by taking advantage of the temperature dependent nature of the TREK-1 channel.

6 male Sprague Dawley rats 450-490g were killed by cervical dislocation, their hearts excised and retrogradely perfused on a Langendorf system. Following stabilization, hearts were subjected to three consecutive diastolic pressures (control: 0-5mmHg, moderate: 20-25mmHg and extreme: 50-55mmHg) at two randomised perfusion temperatures (32°C or 37°C). During manipulation of left ventricular diastolic pressure, endocardial and epicardial monophasic action potentials (MAP) were recorded, and the action potential duration at 80% repolarisation (APD_{80}) calculated. Under control conditions of 0-5mmHg pre-load, the endocardial APD_{80} was 40.3 ±4.2ms, while the epicardial APD_{80} was 45.4 ±4.4ms at 37°C. Decreasing cardiac temperature to 32°C increased both endocardial and epicardial APD_{80} to 46.9 ±3.9ms and 61.1 ±2.7ms respectively. The addition of moderate cardiac pre-load (left ventricular diastolic pressure of 20-25mmHg), did not significantly alter epicardial APD_{80} at either temperature. By contrast, endocardial APD_{80} reduced by 12.2 ±3.2% and 11.6 ±3.7% from control values at 37°C and 32°C respectively.

Extreme left ventricular stretch (50-55mmHg) significantly reduced the APD_{80} in both epicardial and endocardial recordings at 37°C and 32°C. Epicardial APD_{80} reduced by 5.9 ±2.5% and 11.5 ±3.9% relative to control conditions at 37°C and 32°C respectively. Similarly, endocardial APD_{80} decreased by 18.4 ±3.5% and 19.3 ±3.2% at 37°C and 32°C respectively. The reductions in action potential duration observed following extreme stretch at 32°C were not significantly different than those observed at 37°C.

It was concluded that a change in cardiac temperature did not affect the magnitude of reduction in action potential duration (as measured by APD_{80}) following moderate (20-25mmHg) or extreme stretch (50-55mmHg) for either endocardial or epicardial recordings when compared to their control. Since TREK-1 channels are temperature sensitive (inactivating at lower temperatures), these results suggest that non-selective stretch-sensitive cation channels may be more important in modifying action potential duration during stretch than TREK-1 in rat heart.

Immunohistochemical identification of stretch-sensitive two-pore-potassium (TREK) channels in the human heart

S.Y. Yuan, H.P. Zhu and D. Saint, Department of Physiology, School of Molecular & Biomedical Science, University of Adelaide, Adelaide, SA 5005, Australia.

Rhythmic contraction and relaxation of cardiac muscle are determined by a regular cycle of depolarisation and repolarization of cardiac myocytes. Outward movement of potassium ions across the membrane is important for the repolarization and maintenance of resting membrane potential. Potassium channels activated by membrane stretch may contribute to maintenance of normal electrical activity of cardiac myocytes. However, so far there is no evidence for the existence of these channels in human cardiac myocytes. In this study, we examined the existence and location of stretch sensitive potassium (TREK-1 and TREK-2) channels in different regions of human heart using immunohistochemical method. Eight pieces ($5 \times 10 \times 2$ mm^3 for each piece) of human tissue, four fresh atrial appendages and four frozen ventricles taken from patients with coronary bypass surgery and heart transplantation, were processed for immunohistochemistry after fixation and paraffin section. We found that both TREK-1 and TREK-2 immunohistochemical reactivities were observed as bright punctate granules in most atrial and ventricle cardiac myocytes. These are distributed mainly in the cytoplasm and rarely in the center of the nuclear region. Both TREK-1 and TREK-2 immunoreactive granules were found along the surface of cardiac myocyte membranes and the membrane of T-tubules in the cytoplasm (n=4). No connective tissue was labelled. No immunoreactivity was found in negative control preparations after omission of primary antibody. This study demonstrated that TREK-1 and TREK-2 channels are present in human cardiac myocytes. They may play an important role in regulation of human heart electrical behaviour under physiological and diseased conditions.

More than one type of stretch activated channel contributes to the action potential duration in guinea pig

L. Mackenzie, D.R. Kelly and D.A. Saint, Department of Physiology, School of Molecular and Biomedical Science, The University of Adelaide, SA 5000, Australia.

Previously, we provided evidence of the differential involvement of stretch activated channels in the shaping of the action potential through the left ventricular wall of the rat heart. We postulated a role for these channels in the control of dispersion of repolarisation. In this study we aimed to establish if this phenomenon holds for a different species, the guinea pig and also to dissect the contributions of non-selective cation channels (SACs) and the family of stretch activated, 2 pore 4 transmembrane domain, potassium channels (TREK).

We used Langendorff perfused guinea pig heart preparations (N=6) and recorded monophasic action potentials (MAP) simultaneously from the epicardium and the endocardium of the left ventricular free wall under left ventricular end diastolic pressures of 0-5 mmHg (no stretch), 20-25 mmHg (moderate stretch) and 50-55 mmHg (elevated stretch). Hearts were perfused with Hepes buffered Tyrode's solution (pH 7.35-7.37) at 37°C bubbled with oxygen and paced at 4 Hz. This was repeated in the presence of the reported SAC channel blocker streptomycin (80μM). Action potential durations (APDs) at 20, 50 and 80% repolarisation were measured and analysed using general linear model ANOVA followed post hoc by Tukey's pairwise comparisons.

APDs were unchanged compared to control following both moderate and elevated stretch in both the epi- and endocardial layers when measured at 20 and 50% repolarisation. At APD_{80} there was a slight increase in duration although this was not statistically significant. Following blockade of SACs by streptomycin there was a decrease in APDs for 20, 50 and 80% of repolarisation which was significant for both levels of stretch at $APD_{80.}$

These results suggest that both SACs and the family of stretch activated, 2 pore 4 transmembrane domain, potassium channels which we interpret to be TREK contribute to the shaping of the action potential in the guinea pig. We further suggest that the guinea pig may be more susceptible to stretch than the rat as the decrease attributed to TREK was already maximal at 20-25mmHg (moderate stretch).

Fatty acid composition of red blood cell membranes as a marker of human heart membrane phospholipid fatty acids

Mandy L Theiss[1], Salvatore Pepe[2] and Peter L. McLennan[1], [1]Smart Foods Centre, Department of Biomedical Science, University of Wollongong, Wollongong, NSW 2522, Australia and [2]Cardiac Surgical Research Lab, Alfred Hospital & Baker Medical Research Institute, Prahran, VIC 3181, Australia.

Background. Regular intakes of fish or fish oil are associated with low cardiovascular disease morbidity and mortality. A major effect is in reducing sudden cardiac death (Marchioli *et al.*, *2002*). Studies using animals, suggest that the long-chain omega-3 fatty acids, eicosapentaenoic acid (EPA) and docosahexaenoic acid (DHA), have antiarrhythmic and other cardiac effects which are dependent on their incorporation into myocardial membranes (Pepe & McLennan, 1996). The red blood cell (RBC) EPA+DHA content correlates inversely with adverse cardiovascular outcomes and is proposed as a new cardiovascular disease risk factor (Omega-3 Index) (Harris & von Schacky, 2004) on the premise that it reflects the composition of cardiac cells. Animal studies indicate large differences in membrane fatty acid compositions of different tissues.

Objective. To characterise the membrane phospholipid fatty acid composition of human RBC in relation to heart.

Design. Membrane phospholipid fatty acids were extracted from atrial biopsy samples and red blood cells, obtained from cardiac surgery patients (n=10). Mixed venous blood samples were obtained pre-operatively. Biopsy samples were taken from an atrial appendage during open chest surgery. Phospholipid fatty acids were determined by gas chromatography against known standards.

Outcomes. Polyunsaturated fatty acid (PUFA) content of atrial cell membranes was higher (51.13 $\pm$ 0.75%, values are means $\pm$ SE) than RBC (34.88 $\pm$ 0.39%), with PUFA replacing saturated fatty acids. The levels of omega-6 PUFA linoleic acid (LA, 18:2 n-6) 18.89±1.01% and arachidonic acid (AA, 20:4 n-6) 21.32±0.61% were higher in atria than RBC (LA, 6.79±0.34% and AA, 13.96±0.64%). In both atria and RBC, DHA was the major omega-3 fatty acid. Both total omega-3 PUFA and DHA in the atria was highly correlated with RBC EPA+DHA (9.60 $\pm$ 1.14% (range 4.71-11.45%)). Some patients were supplemented with fish oil prior to surgery and had correspondingly higher omega-3 content in both RBC and atria.

Conclusion. The long-chain omega-3 fatty acids EPA and DHA, found in high amounts in fish oil, represent a marker of human atrial omega-3 fatty acid composition and the Omega-3 Index in red blood cells may be a valid marker for human heart composition.

Marchioli, R., Barzi, F., Bomba, E., Chieffo, C., Di Gregorio, D., Di Mascio, R., Franzosi, M.G., Geraci, E., Levantesi, G., Maggioni, A.P., Mantini, L., Marfisi, R.M., Mastrogiuseppe, G., Mininni, N., Nicolosi, G.L., Santini, M., Schweiger, C., Tavazzi, L., Tognoni, G., Tucci, C. & Valagussa, F. (2002) *Circulation*, **105**, 1897-1903.

Pepe, S. & McLennan, P.L. (1996) *Journal of Nutrition*, **126**, 34-42.

Harris, W.S. & von Schacky, C. (2004) *Preventative Medicine*, **39**, 212-220.

Confocal Ca^{2+} imaging of mouse sinoatrial node

Y.K. Ju[1], D.G. Allen[1] and M.B. Cannell[2], [1]School of Medical Sciences, University of Sydney, NSW 2006, Australia and [2]The Faculty of medical and Health Sciences, University of Auckland, Auckland, New Zealand.

Recent studies have demonstrated that intracellular Ca^{2+} plays an important role in cardiac pacemaking (Ju & Allen, 2001). However, the mammalian sinoatrial node (SAN) is a heterogeneous structure and studies on the centre leading pacemaker region suggest that central pacemaker cells do not require the sarcoplasmic reticulum (SR) calcium release for spontaneous activity (Lancaster *et al.*, 2004). In order to study the Ca^{2+} dependent pacemaker mechanisms in different regions of mammalian preparation, we developed a new technique to image Ca^{2+} from intact mouse sino-atrial preparations. Mice (7 -10 weeks) were deeply anaesthetized. The right atrium was opened under a dissecting microscope to expose the crista terminalis, the intercaval area and the interatrial septum as described by Verheijck *et al.* (2001). The preparation was pinned into a sylgard block with a 3×5mm open window that allowed microscopic imaging. The SAN preparation was loaded with the fluorescent Ca^{2+} indicator Fluo-4 AM (10 μM) by incubation in Tyrode solution at 4°C for 5 h. The SAN area was recognized by its anatomic landmarks. 10 mM 2,3–butanedione monoxime (BDM) was used to reduce the motion artifact. The loading of dye into the central region normally was weaker than for peripheral regions for reasons that are unclear. It is known that Na^{+} channels are required for peripheral but not for the central pacemaker activity. Therefore 100 μM lidocaine was added to the perfusate to block any pacemaker type activity from the periphery of the SAN. Spontaneous Ca^{2+} signals from the central SAN were imaged using a confocal microscope (LSM410) in XY and XT modes. We found that the SAN Ca^{2+} signal was modulated by the SR Ca^{2+} release channel modulator caffeine and by ATP. These results show that it is possible to record Ca^{2+} signals from the centre of leading pacemaker region in mouse heart.

Ju, Y.K. & Allen D.G. (2001) *Clinical and Experimental Pharmacology and Physiology* **28**, 703-8.
Lancaster, M.K., Jones, S.A., Harrison, S.M. & Boyett, M.R. (2004) *Journal of Physiology* **556**, 481-494.
Verheijck, E.E., van Kempen, M.J.A., Veereschild, M., Lurvink, J., Jongsma, H.J. & Bouman, L.N. (2001) *Cardiovascular Research* **52**, 40-50.

This work is supported by NH&MRC Australia & HRC New Zealand

Reactive oxygen species generated from the mitochondria and not NAD(P)H-oxidase regulate L-type Ca^{2+} channel function during acute hypoxia in ventricular myocytes

L.C. Hool, H.M. Viola, C.A. Di Maria and P.G. Arthur, School of Biomedical, Biomolecular and Chemical Sciences, The University of Western Australia, WA 6009, Australia.

Hypoxia and the thiol-reducing agent dithiothreitol increase the sensitivity of the L-type Ca^{2+} channel ($I_{Ca\text{-}L}$) to β-adrenergic receptor stimulation. We examined whether NAD(P)H-oxidase regulates cellular production of reactive oxygen species (ROS) and the function of $I_{Ca\text{-}L}$ during hypoxia. Ventricular myocytes were isolated from hearts excised from anaesthetised guinea-pigs as approved by the Animal Ethics Committee of The University of Western Australia and in accordance with the Australian Code of Practice for the Care and Use of Animals for Scientific Purposes (NHMRC). The cells were patch-clamped and current was recorded during exposure to the classic NAD(P)H-oxidase inhibitors apocynin or diphenyleneiodonium (DPI) and increasing concentrations of isoproterenol (Iso). DPI caused an increase in the sensitivity of the channel to Iso similar to that of hypoxia, but apocynin did not. In contrast, the K0.5 for activation of the channel by Iso in the presence of AngII, a potent agonist of NAD(P)H-oxidase during hypoxia was 1.7±0.4 nM which was similar to the K0.5 determined during hypoxia alone (1.6±1.1 nM; NS). We measured cellular production of superoxide anion (O_2^-) using the fluorescent indicator dihydroethidium. Hypoxia was associated with a 41.2±5.2 % decrease in O_2^- (n=21; $P<0.05$). In addition, DPI caused a 21.3±4.7 % decrease in O_2^- (n=16; $P<0.05$). However, O_2^- did not increase when cells were exposed to AngII during hypoxia (n=24) or in room oxygen (n=6). When mitochondria were partially uncoupled with FCCP, there was a 31.3±4.5% decrease in O_2^- (n=23; $P<0.05$) and a significant increase in the sensitivity of $I_{Ca\text{-}L}$ to Iso similar to that of hypoxia (n=7). Accounting for the effect of DPI on $I_{Ca\text{-}L}$, 10μM DPI caused a 67.2±7.3% decrease in oxygen consumption (n=6; $P<0.01$) and 28.8±2.1% decrease in O_2^- in isolated mitochondria (n=4; $P<0.05$) indicating that DPI is not a specific inhibitor of NAD(P)H-oxidase function. Hypoxia decreased O_2^- by 69.3±0.8% in isolated mitochondria (n=4; $P<0.01$). We conclude that a decrease in ROS generated from the mitochondria and not NAD(P)H-oxidase regulates channel function during hypoxia.

Eccentric damage is accentuated in aged dystrophin-deficient EDL muscles from dystrophic mice (MDX)

S. Chan and S.I. Head , School of Medical Sciences, UNSW, NSW 2052, Australia.

Duchenne Muscular Dystrophy (DMD) is second most common fatal inherited condition of humans affecting 1 in 3500 live male births. Due to the large size and high mutation rate of the dystrophin gene, 1/3 of all cases of DMD are the result of a new spontaneous mutation. DMD is characterized by a severe and progressive loss of skeletal muscle and marked CNS and cognitive defects. Death usually occurs in the late teens or early twenties due to the failure of respiratory muscles or cardiac complications. The most commonly used animal model of DMD is the *mdx* mouse in which the long M-isoform of dystrophin is absent from the skeletal musculature. In the *mdx* mouse the proximal limb muscles undergo a process of degeneration which affects 100% of the skeletal muscle fibres in some muscles (Tanabe *et al.*, 1986), the fibres then undergo a process of regeneration and repair. During this period there is a striking change in the morphology of the regenerated *mdx* EDL fibres; up until 15 weeks they are normal cylindrical shaped with no splits or deformities, by 17 weeks 30% of fibres have simple splits and relatively mild deformities, while by 40 weeks in excess of 90% of the EDL fibres have multiple splits and quite striking gross abnormalities (Head *et al.*, 1992). We are hypothesizing that these split, morphologically abnormal fibres are weaker and more susceptible to damage by lengthening contractions of a moderate strain than age matched morphologically normal fibres. We used male *mdx* and male littermate controls from our new line of *mdx* mice (N1F1 *mdx* mice). This provides us with dystrophin-positive controls on an identical genetic background to the dystrophin-deficient animals. This is important because the majority of studies on *mdx* mice use a separate wild type colony as a control and it has been shown that there is a remarkable degree of genetic variation between recently divergent mouse strains (Adams *et al.*, 2005). Animals were killed by an overdose of Halothane (ethics approval granted by UNSW). The EDL muscles were attached at one end to a force transducer and to a servo controlled linear tissue puller at the other end. The muscles were then placed in an organ bath, superfused with oxygenated Krebs and externally stimulated *via* two platinum plates attached to a current amplifier driven by an AM-systems stimulator. The muscles were set to optimal length L_0. The muscles were tetanically stimulated at 100hz, and once the force reached its maximal plateau the lengthening contraction (12, 15 or 20% plus L_0) was given as a ramp, hold and release. The ramp speed was 1mm/sec and the total duration of stimulation was 5 seconds. This protocol was repeated twice at 5 minute intervals to allow recovery from fatigue. The isometric force was recorded after a 20 minute recovery. The muscles were then removed, weighed and single fibres enzymatically (collagenase 1) isolated and viewed on a confocal microscope in order to count the number of split fibres. In aged (45-52 weeks) *mdx* animals, 100% of fibres were split and there was an irreversible 35% ± 9.8 (n=6) drop in isometric force as a result of our lengthening contraction protocol. In contrast, there were no split or deformed fibres in age matched controls, and isometric force was largely unaffected (force drop 3.8%± 4.8% n=5) by this relatively mild eccentric contraction protocol. Numerous previous studies (e.g. Yeung *et al.*, 2003) have demonstrated that dystrophin-deficient fast-twitch muscles are damaged by eccentric contractions; we hypothesise that the extent of the eccentric damage is significantly increased by the presence of deformed fibres.

Adams, D.J., Dermitzakis, E.T., Cox, T., Smith, J., Davies, R., Banerjee, R., Bonfield, J., Mullikin, J.C., Chung, Y.J., Rogers, J. & Bradley A. (2005) *Nature Genetics* 37, 532-6.

Head, S.I., Williams, D.A. & Stephenson, D.G. (1992) *Proceedings of the Royal Society (London) B* 248, 163-169.

Tanabe, Y., Esaki, K. & Numura, T. (1986) *Acta Neuropathologica* 69, 91-95.

Yeung, E., Head, S.I. & Allen, D.G. (2003) *Journal of Physiology (London)* 552(2), 449-458.

Phosphorylation of CSQ affects Ca^{2+} binding and interactions with anchoring protein junctin

N.A. Beard[1], S. Cheung[1], L. Wei[1], M. Varsànyi[2] and A.F. Dulhunty[1], [1]John Curtin School of Medical Research, ANU, Canberra, ACT 0200, Australia and [2]Institut für Physiologische Chemie, Ruhr Universität, Bochum, Germany.

Depolarisation of the sarcolemma triggers Ca^{2+} release through ryanodine receptor (RyR) calcium release channels in the sarcoplasmic reticulum (SR) of skeletal muscle. Calsequestrin (CSQ) is the major Ca^{2+} binding protein found within the SR, and binds Ca^{2+} with a high capacity and moderate affinity. Recent studies have shown that CSQ also regulates RyRs. The best studied mechanism of CSQ-RyR interaction is indirect, thought to be mediated by anchoring proteins triadin and junctin and results in RyR inhibition (Szegedi *et al.*, 1999; Beard *et al.*, 2002). The relative importance of triadin and junctin in facilitating the interaction with the RyR is not clear, nor is the role *in vivo* of CSQ phosphorylation on the interaction between triadin, junctin and the RyR. Given that CSQ is isolated in both a phosphorylated and dephosphorylated form, it is conceivable that a CSQ phosphorylation/dephosphorylation cycle is important in regulating the RyR. Our hypothesis is that as the site of CSQ phosphorylation is believed to be close to the putative Ca^{2+} binding site, and triadin and junctin binding sites, that changes in phosphorylation may modify Ca^{2+} binding capacity and the ability of CSQ to interact with triadin and/or junctin.

We have investigated the effects of CSQ phosphorylation on CSQs role as a Ca^{2+} binding protein and regulator of the native RyR. Rabbit skeletal CSQ cDNA was subcloned into a pGex 5X-1 vector (containing a glutathione-*S*-transferase tag), transformed and expressed in *Escherichia coli* BL21(DE3) cells. CSQ was phosphorylated and dephosphorylated according to established methods (Cala & Jones, 1991).

We found that the Ca^{2+} binding capacity was significantly reduced in dephosphorylated CSQ (deP-CSQ), compared with phosphorylated CSQ (P-CSQ) over a range of [Ca^{2+}] from 100 nm – 5 mM. This was most evident at the physiological free [Ca^{2+}] (1 mM) and at 5 mM Ca^{2+} (a concentration shown to dissociate CSQ from the native RyR). Despite these changes in binding capacity, both P-CSQ and deP-CSQ caused similar significant inhibition of the native RyR (at 1 mM luminal Ca^{2+}; Beard *et al.*, 2005). As the putative major Ca^{2+} binding region and site of CSQs interaction with triadin and junctin are presumed identical (residues 354-367), we investigated what effects P-CSQ/deP-CSQ had on its interactions with triadin and junctin. Using CSQ-GST fusion protein affinity chromatography, we found that under close to physiological conditions (150 mM NaCl, 1 mM Ca^{2+}), both P-CSQ and deP-CSQ bound triadin and junctin. Not surprisingly, under conditions known to completely dissociate CSQ from the native RyR (5 mM Ca^{2+}), neither P-CSQ nor deP-CSQ interacted with a significant amount of triadin or junctin. Curiously, at low luminal Ca^{2+} (100 nM), CSQ binding to these two anchoring proteins was phosphorylation-dependent. P-CSQ bound significant amounts of both triadin and junctin, whilst deP-CSQ was found only to interact with triadin, but not with junctin. In experiments where 100 nM luminal Ca^{2+} was used to depolymerise P-CSQ and deP-CSQ from a solubilized SR sample, a significant proportion of both forms of CSQ remained tethered close to the RyR/triadin/junctin complex. The combination of these results suggests that an interaction with junctin is not required to tether CSQ close to the native RyR.

These results show firstly, that CSQ dephosphorylation reduces the ability of CSQ to bind Ca^{2+}. Although this does not affect overall CSQ regulation of the RyR, subtle effects of altering CSQs phosphorylation status on channel gating, or CSQs ability to act as a luminal Ca^{2+} sensor remain to be investigated. Secondly, these results illustrate that triadin, but not junctin, is essential for association of CSQ with the native RyR. Further investigation on whether the alteration in junctin binding results in altered regulatory effects on the native RyR may elucidate a specific role of junctin and the potential P-CSQ/deP-CSQ cycle on SR Ca^{2+} release. Thirdly, the results show that conformational changes that alter Ca^{2+} binding capacity do not necessarily alter CSQ binding to triadin and junctin and therefore the specific residues which comprise both the major Ca^{2+} binding site and triadin/junctin binding sites are not identical.

Beard, N.A., Casarotto, M.G., Wei, L., Varsányi, M., Laver, D.R. & Dulhunty, A.F. (2005) *Biophysical Journal* **88**, 3444-3454.

Beard, N.A., Sakowska, M.M., Dulhunty, A.F. & Laver, D.R. (2002) *Biophysical Journal* **82**, 310-320.

Cala, S.E. & Jones, L.R. (1991) *Journal of Biological Chemistry* **266**, 391-398.

Szegedi, C., Sarkozi, S., Herzog, A., Jona, I. & Varsanyi, M. (1999) *Biochemical Journal* **337**, 19-22.

A calsequestrin polymer is necessary for the Ca^{2+} binding protein to regulate RyR channels

L. Wei, N.A. Beard and A.F. Dulhunty, John Curtin School of Medical Research, Australian National University, Canberra, ACT 0200, Australia.

Calsequestrin (CSQ) forms a complex with the Ca^{2+} release channel ryanodine receptor (RyR) and anchoring proteins, triadin (Tri), and junctin (Jun) in the lumen of the sarcoplasmic reticulum (SR) of skeletal and cardiac muscles. CSQ acts to both regulate the RyR, and buffer the $[Ca^{2+}]_{free}$ inside the SR at 1 mM (Beard *et al.*, 2004). CSQ requires a compact structural conformation to achieve high capacity Ca^{2+} binding (He *et al.*, 1993). CSQ is thought to undergo a self-polymerisation as local $[Ca^{2+}]$ increases, and is believed to form a polymer at the physiological $[Ca^{2+}]$ (1 mM) in the SR. Our aim was to determine whether the CSQ polymer and its regulatory interaction within the complex would be disrupted and whether CSQ would be dissociated from the quaternary complex, when the intraluminal $[Ca^{2+}]$ falls to a low level at which CSQ is thought to be depolymerised. To achieve this, we examined the effects of low luminal Ca^{2+} on CSQs ability to regulate the RyR and correlated these effects with known Ca^{2+}-dependent changes in CSQ structure.

New Zealand male white rabbit were euthanized by a captive bolt and back and leg muscle used to prepare heavy SR vesicles. Heavy SR vesicles were reconstituted into artificial planar lipid bilayers, which separate two chambers, *cis* (cytoplasmic) and *trans* (luminal). *Trans* $[Ca^{2+}]$ was kept at 1 mM during incorporation and then lowered to 100 nM by the addition of BAPTA or EGTA. Channel activity was recorded at positive and negative potentials. To determine the effect of $[Ca^{2+}]$ on CSQ association with the RyR/Tri/Jun complex, SR vesicles were solubilised in 0.5% triton X-100, followed by an ultracentrifugation and resuspended in a solution containing 1 mM Ca^{2+}. The suspension was divided to three fractions and incubated at 4°C for 1 h in 1 mM, 1 μM and 100 nM Ca^{2+} after adjustment of $[Ca^{2+}]$ by BAPTA, prior to a second centrifugation. Resultant pellets and supernatants were subjected to SDS-PAGE and immunoblot analysis.

In single channel studies, a sudden delayed increase in activity was observed after the native RyR was exposed to low luminal Ca^{2+} (100 nM) for ~3 min. Returning *trans* $[Ca^{2+}]$ to 1 mM did not fully reverse the increase in activity to control levels, but addition of 16 μg/ml of exogenous CSQ to the *trans* chamber completely restored control channel activity. These changes were similar to those seen with dissociation of CSQ from the RyR/Tri/Jun, with high luminal ionic strength or Ca^{2+} (Beard *et al.*, 2004), but a longer exposure time was required before the sudden increase in activity was observed. The levels of CSQ in the membrane pellet of solubilised junctional face membrane (containing the RyR/Tri/Jun/CSQ complex) exposed to different $[Ca^{2+}]$, were compared with levels found in the original membrane fractions, to determine if CSQ was dissociated from the membrane. Increasing amounts of CSQ were dissociated from the membrane pellet as $[Ca^{2+}]$ fell, with 8.6%, 35.8% and 63% of the total CSQ dissociated by 1 mM, 1μM and 100 nM Ca^{2+}, respectively. This is in contrast to ~100% dissociation with high ionic strength or high Ca^{2+}. Additional single channel experiments showed that the response of RyRs associated with depolymerised CSQ to changes in luminal Ca^{2+} between 100 nM to 1 mM was typical of that seen in channels in which CSQ was fully dissociated.

Since CSQ is depolymerised with low $[Ca^{2+}]$ but retains its ability to bind to triadin and junctin (Shin *et al.*, 2000), we suggest that the CSQ remaining associated with the junctional face membrane was bound to triadin and junctin and that the dissociated CSQ was depolymerised and dissociated from the residual bound CSQ. Channel data suggests that the delayed RyR activation reflects depolymerisation and dissociation of CSQ not bound to triadin and junctin. The longer delay before the sudden increase in channel activity after exposure to low Ca^{2+} suggest a different physical process to the dissociation from triadin and junctin seen with high ionic strength and high Ca^{2+}. The results further suggest that the residual CSQ remaining associated with the RyR/Tri/Jun complex after depolymerisation was unable to regulate RyR activity in the normal manner until it formed a polymer with the excess exogenous CSQ. Therefore we concluded that a CSQ polymer is required for the calcium binding protein to regulate the RyR via triadin and junctin.

Beard, N.A., Laver D.R. & Dulhunty, A.F. (2004) *Progress in Biophysics and Molecular Biology* **155,** 33-69.

He, Z., Dunker, A.K., Wesson C.R. & Trumble, W.R. (1993) *Journal of Biological Chemistry* **268,** 24635-24641.

Shin, D.W., Ma, J. & Kim D.H. (2000) *FEBS Letters* **486,** 178-182.

Digoxin and exercise effects on Na^+,K^+-pump activity, content, isoform gene and protein expression in human skeletal muscle

X. Gong[1], A. Petersen[1], S. Sostaric[1], C. Goodman[1], D. Cameron-Smith[2], R. Snow[2], K. Murphy[1], K. Carey[2], J. Aw[3], H. Krum[3] and M. McKenna[1], [1]School of Human Movement, Recreation and Performance, Centre for Ageing, Rehabilitation, Exercise and Sport, Victoria University, Melbourne, VIC 8001, Australia, [2]School of Exercise Science and Nutrition, Deakin University, Melbourne, VIC 3125, Australia and [3]Department of Epidemiology and Preventive Medicine, Monash University, Alfred Hospital, Melbourne, VIC, Australia.

Digoxin is a specific inhibitor of the Na^+,K^+-pump and is used to treat patients with severe heart failure. In these patients, digoxin binds and blocks ~13% of Na^+,K^+-pumps in skeletal muscle and exacerbates muscle K^+ loss during exercise. Furthermore in heart failure patients there is no compensatory upregulation of Na^+,K^+-pump with chronic digitalisation. We have shown that exercise impairs Na^+,K^+-pump activity, whilst in isolated rat muscles, Na^+,K^+-pump inhibition leads to early muscle fatigue (Clausen, 2003). Hence, Na^+,K^+-pump function is likely to be important for skeletal muscle performance. However, the effects of digoxin on Na^+,K^+-pump content, activity, protein abundance or isoform expression in skeletal muscle of healthy individuals are unknown and were investigated here.

Ten active, but not well-trained healthy volunteers (9 M, 1 F) gave written informed consent. Exercise tests were performed after taking digoxin (DIG, 0.25 $mg.d^{-1}$) or a placebo (CON) for 14 d, in a randomised, counterbalanced, cross-over, double blind design, with trials separated by 4 weeks. Subjects performed incremental cycle ergometer exercise to measure VO_{2peak} and to determine 33, 67 and 90% VO_{2peak} work rates. On d 14 subjects completed 10 min cycling at each of 33% and 67% VO_{2peak}, then to fatigue at 90% VO_{2peak}. Muscle biopsies taken at rest, after 67%, 90%VO_2 peak and 3 h recovery were analysed for Na^+,K^+-pump content (^{3}H-ouabain binding site), maximal activity (3-*O*-methyfluorescein phosphatase, 3-*O*-MFPase), isoform protein abundance and mRNA expression. The Na^+, K^+-pump isoform (α_1-α_3, β_1-β_3) protein contents were measured on muscle extracts, using specific antibodies and western blotting, with isoform mRNA expression determined with real-time RT-PCR analysis.

Serum digoxin was 0.7±0.2 nM at d 13 and 0.8±0.2 nM at d 14 (Mean±SD). Despite this, muscle maximal Na^+,K^+-pump activity was unchanged by digoxin. However, Na^+,K^+-pump activity was decreased after exercise, by 13% and 11% at fatigue and 3 h post-exercise, compared to rest, respectively (P<0.05). Furthermore, there was no change in the Na^+,K^+-pump content with either digoxin or exercise (Rest Digoxin 373±95, Rest Placebo 368±75 pmol.g wet $weight^{-1}$). No significant change occurred with digoxin for mRNA expression of any of the α_1, α_2, α_3, β_1, or β_3 isoforms. However, digoxin increased the mRNA expression of the total α mRNA (sum of α_1, α_2, α_3) and the total β mRNA (sum of β_1 and β_3) at rest by 1.9- and 1.8-fold, respectively (P<0.05), suggesting an effect of digoxin on Na^+,K^+-pump gene expression. An exercise effect was observed on α_3 mRNA expression, being 2.1-and 2.4-fold higher at 3 h post-exercise than during exercise at 67% VO_2peak and fatigue, respectively (P<0.05). Similarly, β_3 mRNA expression at 3 h post-exercise was increased by 1.8-, 1.4- and 1.6-fold, compared to rest, 67% VO_2peak exercise and fatigue, respectively (P<0.05). Digoxin did not alter the protein abundance of any isoform in resting muscle. However, at 3 h post-exercise, the protein abundance was greater with digoxin than in placebo for both α_2 and β_3 (P<0.05). The β_1 protein expression was increased at 3 h post-exercise by 2.2-and 1.5-fold compared to during exercise at 67% VO_2peak and fatigue, respectively (P<0.05). Similarly, β_3 protein expression was increased at 67% VO_2peak and 3 h post-exercise compared to rest, by 1.5-and 1.6-fold, respectively (P<0.05).

In summary, digoxin treatment had only minimal effects on muscle Na^+,K^+-pumps in healthy individuals. Whilst Na^+,K^+-pump content, activity or isoform protein expression at rest were unchanged, the subunit total mRNA expression was increased with digoxin and a greater post-exercise protein abundance was found with digoxin for α_2 and β_3. The lack of reduction in pumps with digitalisation in healthy muscles suggests either that pumps were upregulated and/or that digoxin dissociation was increased.

Clausen, T. (2003) *Physiolgical Reviews* **83**, 1269-324.

Funded by NH&MRC

Reduced long-term depression is recovered in aging mdx cerebellar Purkinje cells

J.L. Anderson, S.I. Head
and J.W. Morley, School of Medical Sciences, UNSW, NSW 2052, Australia.

Duchenne muscular dystrophy (DMD) is characterized primarily by a loss of skeletal muscle and marked CNS and cognitive defects (Anderson *et al*,, 2002). It is known that DMD is due to the mutation of a gene which produces the protein dystrophin, of which there are seven identified isoforms, expressed in a range of tissues including brain. In the cerebellum an isoform of dystrophin is found exclusively in Purkinje neurons and is selectively localised in post-synaptic regions of GABAergic synapses. We have previously demonstrated (Anderson *et al*,, 2004) a deficit in long-term depression (LTD) in cerebellar Purkinje cells in the *mdx* mouse (an animal model of DMD) compared to controls at 3 months of age. mdx mice. --> In the present study we investigated LTD and short-term plasticity at the parallel fibre to Purkinje cell synapse in cerebellar brain slices from ageing (6-12 months) control and *mdx* mice. Mice were anaesthetised with halothane, decapitated, cerebellum removed, bisected, placed in ice-cold aCSF and sagittal slices (250μM) cut. Individual Purkinje cells were visualised using a 40× immersion lens and IR-DIC optics. Intracellular electrodes (~120MΩ) filled with potassium acetate were used and a stimulating electrode was placed in the molecular layer of the slice (<250μM from the cell under study). We found that the deficit in LTD which we reported (Anderson *et al*,, 2004) in *mdx* mice at 3 months of age was no longer evident in aging *mdx* mice, and that these cells showed a long lasting and robust LTD. In addition, there were no differences in short-term plasticity between the ageing control and *mdx* mice.

Anderson, J.L., Head, S.I., Rae, C. & Morley, J.W. (2002) *Brain* **125**, 4-13.
Anderson, J.L., Head. S.I. & Morley, J.W. (2004) *Brain Research* **1019**, 289-92.

Differential action of ω-conotoxins CVID and CVIB on voltage-gated calcium channels in rat sensory neurons

L.M. Motin, R.J. Lewis and D.J. Adams, School of Biomedical Sciences, University of Queensland, Brisbane, QLD 4072, Australia.

Selective antagonists of voltage-gated calcium channels (VGCCs) are of considerable interest both as research tools and potential therapeutic agents. The selectivity of VGCC antagonists is essential for dissecting the various Ca^{2+} channel types underlying the whole-cell Ca^{2+} current whereas potency and reversibility play an important role in the use of a VGCC antagonist as a pharmaceutical agent. ω-Conotoxins GVIA, MVIIA and MVIIC have been used routinely as selective blockers of N- and P/Q-types of VGCCs in excitable cells. However, the newly discovered ω-conotoxins from *Conus catus*, CVID has been shown to have the highest selectivity for N-type over P/Q-type VGCCs among the other N-type selective VGCC antagonists (Lewis *et al.*, 2000). The present study investigated the selectivity, potency and reversibility of action of ω-conotoxins CVID and CVIB in isolated sensory neurons dissociated from rat dorsal root ganglia (DRG) and on recombinant VGCCs expressed in *Xenopus* oocytes. Bath application of either CVID or CVIB inhibited depolarization-activated whole cell Ba^{2+} currents in DRG neurons with pIC_{50} values of -8.12 ± 0.05 and -7.64 ± 0.08, respectively. The block of Ba^{2+} currents in DRG neurons by CVID appeared to be irreversible after >30 min washout whereas Ba^{2+} currents exhibited rapid recovery from block by CVIB (>80% within 3 min). ω-Conotoxin CVIB inhibited more of the whole-cell Ba^{2+} current in DRG neurons than CVID and the recoverable component of the Ba^{2+} current inhibited by CVIB was mediated by the N-type VGCC. The potency of CVID and CVIB block of N- and P/Q-type VGCCs was compared with the ω-conotoxins, GVIA, MVIIA and MVIIC. ω-Conotoxins GVIA and MVIIA inhibited Ba^{2+} currents in DRG neurons to a similar degree as CVID. The residual current amplitude obtained in the presence of maximally effective concentrations of the ω-conotoxins was: GVIA, 54 ± 0.2%; MVIIA, 41 ± 0.04% and CVID, 34 ± 1%. The residual current after block by CVIB was 3 ± 5% of control level reflecting non-selective N- and P/Q- action of the toxin. ω-Conotoxin CVIB reversibly inhibited Ba^{2+} currents mediated by N- ($Ca_v2.2$) and P/Q- ($Ca_v2.1$) type VGCCs expressed in *Xenopus* oocytes. The $\alpha_2\delta_1$ auxiliary subunit coexpressed with $Ca_v2.2$ and $Ca_v2.1$ reduced the potency of CVIB as reported previously for CVID at recombinant N-type VGCCs (Mould et al., 2004). The present study demonstrates that ω-conotoxins CVID and CVIB can be successfully used for pharmacological isolation of N- and P/Q- components of the Ca^{2+} conductance in rat DRG neurons. CVID selectively and irreversibly blocked the N-type component of the whole cell Ba^{2+} current in DRG neurons but blocked reversibly the recombinant N-type ($Ca_v2.2$) VGCC. In contrast, CVIB blocked reversibly the N-type component and blocked irreversibly P/Q- component of the whole cell Ba^{2+} current in DRG neurons. ω-Conotoxins CVID and CVIB may be useful as antagonists of N- and P/Q-type VGCCs in sensory neurons involved in processing primary nociceptive information.

Lewis, R.J., Nielsen, K.J., Craik, D.J., Loughnan, M.L., Adams, D.A., Sharpe, I.A., Luchian T., Adams, D.J., Bond, T., Thomas, L., Jones, A., Matheson, J-L., Drinkwater, R., Andrews, P.R. & Alewood, P.F. (2000) *Journal of Biological Chemistry* **275**, 35335–35344.

Mould, J., Yasuda, T., Schroeder, C.I., Beedle, A.M., Doering, C.J., Zamponi, G.W., Adams, D.J. and Lewis, R.J. (2004) *Journal of Biological Chemistry* **279**, 34705-34714.

Evidence from collision experiments that onset chopper neurons in the guinea pig cochlear nucleus receive excitatory input from centrifugal collaterals

D. Robertson and W.H.A.M. Mulders, The Auditory Laboratory, Discipline of Physiology, School of Biomedical Biomolecular and Chemical Sciences, The University of Western Australia, Crawley, Western Australia 6009, Australia.

In mammals, centrifugal pathways from the superior olivary complex to the cochlea, send collateral projections to the first brainstem nucleus, the cochlear nucleus. The action of these collateral pathways needs to be taken into account in any attempt to understand the role of the centrifugal olivocochlear system in auditory processing. To date however there is only incomplete understanding of the neuronal targets of the collaterals and of their synaptic effects (Benson & Brown, 1990; Mulders *et al.*, 2003; Mulders *et al.*, 2002). We have observed in guinea pigs that electrical stimulation at the floor of the IVth ventricle (the site of passage of the centrifugal axons as they ascend from the superior olivary complex), gives rise to short-latency action potentials in well-characterized onset chopper neurons. The nature of these electrically-evoked spikes however, is unclear, since they show an ability to follow quite high rates of electrical stimulation, perhaps consistent not with an excitatory synaptic drive from centrifugal collaterals, but rather, antidromic spikes initiated in the dorsally-ascending axons of the onset chopper neurons. We set out to distinguish between these possibilities by using classical collision techniques to distinguish antidromic from synaptically-driven action potentials. The experiments were performed in guinea pigs anaesthetized with intraperitoneal sodium pentobarbitone (30mg/kg) and 0.15ml intramuscular Hypnorm (fluanisone, 10mg/ml and fentanyl citrate, 0.315mg/ml). During electrical stimulation, the animals were paralyzed by intramuscular administration of Pancuronium. Heart rate was continuusly monitored and regular supplementary doses of both anaesthetics were given throughout the experiment. Data from a small number of well-characterized onset chopper neurons, showed that action potential collision only occurred at delays that were either the same as, or shorter than the delay between shocks and shock-evoked spikes in the same neurons. This result is inconsistent with the electrically-evoked spikes being antidromic and strongly suggests that the axon collaterals of olivocochlear neurons exert excitatory synaptic effects on onset chopper neurons. Furthermore, the robust nature of the spiking to high rates of shocks suggests that the synaptic connection is a powerful one, giving rise to strong and comparatively secure excitation of this class of cochlear nucleus neurons.

Benson, T.E. & Brown M.C. (1990) *Journal of Comparative Neurology* 295: 52-70.
Mulders, W.H., Paolini, A.G., Needham, K. & Robertson, D. (2003) *Hearing Research* 176: 113-121.
Mulders, W.H., Winter I.M. & Robertson, D. (2002) *Hearing Research* 174: 264-280.

P2Y receptor activation inhibits the formation and proliferation of primary mouse sub-ventricular-derived neurospheres

M.R. Stafford, P.F. Bartlett and D.J. Adams, School of Biomedical Sciences and The Queensland Brain Institute, University of Queensland, Brisbane QLD 4072 Australia.

Purinergic receptors mediate a variety of biological effects in response to extracellular nucleotides. In the brain, astrocytes and neurovascular endothelial cells release nucleotides such as ATP and may have regulatory roles in the stem cell micro-environment. Extracellular ATP also mediates Ca^{2+} wave propagation between astrocytes. Further, a correlation between Ca^{2+} wave intensity and cortical neuronal production in the ventricular zone of the embryo suggests a potential role for extracellular ATP and Ca^{2+} waves in early neurogenesis. In the present study we show that (i) sub-ventricular zone (SVZ) stem cells express purinergic receptors, (ii) ATP evokes intracellular Ca^{2+} transients in SVZ-derived neurospheres, and (iii) purinergic agonists can affect primary neurosphere formation and proliferation. $HSA^{lo}PNA^{lo}$ stem cells were purified from the SVZ of adult mice using flow cytometry. The stem cell population expressed mRNA for P2Y1, 2, 6, 12 and 14 receptor subtypes. In primary neurospheres loaded with Fura-2AM, ATPγS (1-30 μM) and ADPβS (1-30 μM) evoked Ca^{2+} transients in the presence and absence of external Ca^{2+}. Transients were reversibly attenuated by PPADS (20 μM) and completely abolished by the P2Y1 antagonist MRS2179 (30 μM), suggesting the presence of functional metabotropic P2Y1 receptors. To study purinergic effects on sphere formation, single cell suspensions derived from primary SVZ tissue were treated with purinergic agonists/antagonists and grown under sphere forming conditions. ATPγS and ADPβS (10-30 μM) but not UTP, UDP, UDP-glucose or αβ methylene ATP (100 μM) reduced both the size and frequency of primary neurospheres. This inhibitory effect was partially antagonized by MRS2179 (30 μM) and completely reversed by the P2Y12 antagonist MRS2395 (10 μM). Taken together, these data demonstrate that ATP and ADP evoke P2Y1 mediated Ca^{2+} transients in SVZ-derived neurospheres and that the inhibitory effect of adenine nucleotides on neurosphere formation and proliferation involves P2Y1 and P2Y12 receptor activation. Modulation of either stem cell proliferation or differentiation by purinergic receptor mediated G-protein signalling pathways may therefore represent a potential modulatory mechanism within the stem cell niche.

Protein kinase A inhibits cell growth induced by overexpression of IK channels

C.J. Fowler, K. Ngui, B. Hunne, D. Poole, J.B. Furness and C.B. Neylon, Department of Anatomy and Cell Biology, The University of Melbourne, VIC 3010, Australia.

Intermediate-conductance (IK) potassium channels have been shown to play a key role in the proliferation of different cell types. Blockers of IK channels are effective in inhibiting the growth of lymphocytes, proliferative smooth muscle cells and various cancer cells. We have shown previously that the IK channel is regulated by cAMP-dependent protein kinase (PKA). As the PKA pathway is generally thought to be growth inhibitory, we wished to examine whether PKA can modulate the influence of IK channel activity on cell growth.

An IK-expressing stable cell line was generated in HEK293 cells. The V5 antibody epitope was engineered into the rat IK cDNA, which was transfected into HEK293 cells and cultured in the presence of G418. Western blotting of cell extracts revealed an anti-V5 immunoreactive band at 43kDa which was not present in untransfected HEK293 cells. This band corresponds to the recombinant IK channel subunit. For proliferation assays, cells were seeded at 50,000 cells per 35mm diameter dish and cultured up to 5 days in DMEM containing 10% foetal bovine serum. Cells were counted in duplicate using a haemocytometer.

The IK-expressing stable cell line proliferated at a significantly faster rate compared to the untransfected control HEK293 cells. This enhanced cell growth was completely inhibited by the IK channel antagonist, clotrimazole (10μM). To determine the effect of PKA, cells were exposed to the adenylate cyclase activator forskolin (10μM) during the rapid growth phase. Forskolin prevented the enhanced growth of IK channel-overexpressing cells but had no effect on proliferation of untransfected HEK293 cells.

Serine 332 on the IK channel is a strong PKA consensus site (Neylon *et al.*, 2004). To determine whether the inhibition of cell growth by PKA was due to direct phosphorylation of S332, we generated a stable cell line overexpressing IK channels containing the S332A mutation. Cells overexpressing the S332A mutant grew at a similar rate to those overexpressing wild type IK channels. However, the inhibition of cell proliferation by forskolin was attenuated. Forskolin produced only 30% inhibition of the enhanced growth of cells overexpressing S332A-IK channels, compared to 100% for wild type IK channels.

We conclude that PKA can prevent the influence of IK channels on cell growth, and this effect is mediated partially through direct phosphorylation of S332 on the IK channel.

Neylon, C.B., D'Souza, T., & Reinhart, P.H. (2004) *Pflügers Archiv* **448**, 613-620.

Post-transcriptional regulation of CFTR protein expression by 5′untranslated region encoded regulatory elements

S-J. Conroy, W.L Davies and A.E.O. Trezise, School of Biomedical Science, The University of Queensland, QLD 4072, Australia.

Cystic fibrosis is a common, fatal genetic disease caused by mutations in the *cystic fibrosis transmembrane conductance regulator* gene (CFTR). CFTR encodes for a cAMP regulated chloride channel present in epithelial, cardiac and neuronal tissues, the loss of which impairs electrolyte transport across epithelial cells resulting in cystic fibrosis (CF) disease. CFTR expression is tightly controlled by a combination of transcriptional, post-transcriptional, translational and post-translational regulatory mechanisms, resulting in complex spatial, temporal, and pathological expression patterns. However, the regulatory mechanisms controlling CFTR expression *in vivo* are not well understood.

Despite the importance of the transcriptional regulation of CFTR, we have recently shown that CFTR is subject to post-transcriptional regulation through the action of upstream open reading frames (uORFs) encoded within the CFTR 5′untranslated region (5′UTR) (Davies *et al.*, 2004). We have investigated a highly conserved uORF present in the 5′UTR of the predominant epithelial of CFTR mRNA isoform. Evidence for uORF involvement in post- transcriptional regulation has been found in many eukaryotic genes, and has been attributed to disruption of ribosome scanning during translation, thereby modulating translation initiation at the main coding region.

We investigated the functional importance and mechanism of action of the 5′UTR in CFTR post-transcriptional regulation. We generated a series of expression constructs linking wildtype and mutant rabbit CFTR 5′UTR sequences to the firefly luciferase reporter gene. Following transfection of HT29 and CHO cells, measurement of luciferase activity indicated the effect of CFTR 5′UTR encoded regulatory elements on translation of the main coding region. For each construct, triplicate independent transfections were performed and co-transfection with renilla luciferase controlled for minor differences in transfection efficiency.

It was found that the wildtype CFTR 5′UTR (uORF present) supported translation of the main coding region at just 50% of the level produced by the positive control (beta-globin) 5′UTR, suggesting the presence of negative regulatory elements. Mutations that increase translation of the uORF result in a further 50-70% decrease in translation of the main coding region. In contrast, the elimination of the uORF translation, by truncation of the 5′UTR or direct mutation of the uORF, produces a 50% increase in translation of the main coding region compared to the wildtype CFTR 5′UTR. Overall the effect of each 5′UTR construct was very similar in both CFTR expressing (HT29) and non-expressing (CHO) cell lines. However, some small differences are indicative of tissue-specific *trans*-acting modulatory factors. These results identify a new mechanism of CFTR regulation, confirming the importance of 5′UTR regulatory elements in modulation of CFTR expression.

Davies, W.L., Vandenberg, J.I., Sayeed, R.A. & Trezise, A.E. (2004) *Biochemical and Biophysical Research Communications* **319**, 410-418.

Nedd4-2, ClC-5 and albumin endocytosis in the proximal tubule: a role for SGK-1?

D.H. Hryciw[1], J. Ekberg[1], A. Lee[1], I.L. Lensink[2], S. Kumar[2], W.B. Guggino[3], D.I. Cook[4], C.A. Pollock[5] and P. Poronnik[1], [1]School of Biomedical Sciences, University of QLD, Brisbane, QLD 4072, Australia, [2]Hanson Institute, IMVS, Adelaide, SA 5000, Australia, [3]Department of Physiology, School of Medicine, Johns Hopkins University, Baltimore, MD 21205, USA, [4]Department of Physiology, University of Sydney, NSW 2006 Australia, and [5]Kolling Institute, RNSH, University of Sydney, NSW 2065, Australia.

Retrieval of urinary albumin by the proximal tubule is achieved by receptor-mediated endocytosis that involves a macromolecular complex that includes megalin/cubulin receptor, the Cl^- channel ClC-5, Na-H exchanger isoform 3 (NHE3) and v-H^+-ATPase. Defects in this uptake pathway result in increased albumin excretion, albuminuria and eventually nephropathy. Genetic defects in ClC-5 in patients with Dents disease lead to persistent proteinuria. ClC-5 knockout mice also have proteinuria, demonstrating a key role for ClC-5 in this process. ClC-5 is expressed at the apical cell membrane of the proximal tubule and we have been investigating the molecular basis for the role of ClC-5 in albumin uptake. ClC-5 has a large intracellular C-terminus that can potentially act with numerous regulatory proteins. Previously it has been demonstrated that the cell surface expression of ClC-5 can be regulated by an ubiquitin ligase, WWP2. In the current study we showed that Nedd4-2 interacts with ClC-5 and that this interaction is an essential component of constitutive albumin uptake (Hryciw *et al.*, 2004). We also investigated whether serum- and glucocorticoid-inducible kinase (SGK-1) plays a role in this endocytic process.

We first used Glutathione S transferase (GST) fusion pulldowns to show that C-terminus of ClC-5 bound both Nedd4 and Nedd4-2. The Xenopus oocyte expression was then used to show that Nedd4-2 but not Nedd4 reduced ClC-5 currents in a manner that was dependent on an intact proline rich motif containing a tyrosine (PY) in ClC-5. Using luminescence detection of an influenza hemagglutinin-HA-epitope-tagged ClC-5, the decrease in ClC-5 currents was confirmed to be due to a reduction in cell surface levels of ClC-5. Acute exposure of opossum kidney (OK) cells to albumin resulted in a rapid increase in the protein levels of both ClC5 and Nedd4-2 and an increase in proteasome activity. Conversely, inhibition of the proteasome or silencing of endogenous Nedd4-2 in OK cells caused significant decreases in albumin endocytosis. These data indicate that constitutive albumin uptake involves the upregulation of the ubiquitin/proteasome system

In the cortical collecting duct, it is hypothesized that SGK inhibits the action of Nedd4-2 on ENaC. We therefore investigated the role of SGK-1 on albumin uptake in OK cells. Overexpression of wildtype SGK-1 resulted in a significant increase albumin endocytosis 114 ± 3.5%; n = 4; P Our data clearly demonstrate that, similar to the reabsorption of Na^+ by the cortical collecting duct, that the constitutive uptake of albumin involves ubiquitin ligases, the proteasome and SGK-1. However, it appears that the effects of SGK-1 do not involve either Nedd4-2 or ClC-5 in OK cells. These data highlight the complex nature of the endocytic process that mediates the retrieval of albumin from the glomerular filtrate.

Hryciw DH, Ekberg J, Lee A, et al. (2004) Journal of Biological Chemistry, 279:54996-5007.

Na^+ H^+ exchanger regulatory factor 2 (NHERF-2) is a scaffold for the plasma membrane Ca^{2+} ATPase (PMCA)

W.A. Kruger[1], G.R. Monteith[2], L. Tongpao[1] and P. Poronnik[1], [1]School of Biomedical Sciences, The University of Queensland, St Lucia, QLD 4072, Australia and [2]School of Pharmacy, The University of Queensland, St Lucia, QLD 4072, Australia.

Resting cytosolic Ca^{2+} levels are maintained at nanomolar levels by the sequestration of Ca^{2+} into intracellular stores or the extrusion of Ca^{2+} across the plasma membrane by the PMCA. Despite the ubiquitous distribution of PMCA and its pivotal role in Ca^{2+} signalling, little is known about how PMCA activity is regulated during G protein coupled receptor signalling. There are 4 isoforms of PMCA (1-4) and many splice variants of all isoforms have been identified and all PMCA-b splice variants have a consensus class 1 PSD-95/Dlg/Zo-1 (PDZ) binding motif (Strehler *et al.*, 2001). Protein-protein interactions mediated by PDZ modules are now recognized as playing a key role in spatially constraining many ion channels and transporters into signalling complexes in membrane microdomains (Pawson *et al.*, 1997). Previously, PMCA 2b has been reported to interact with NHERF-2 in a heterologous expression system (DeMarco *et al.*, 2003). This study investigated whether PMCA interacts with NHERF-2 in a native epithelial cell and the physiological significance of this interaction in terms of G-protein mediated Ca^{2+} signalling via the muscarinic M3 receptor.

This study used the polarised epithelial HT29 cell line which expresses only the M3 isoform of the muscarinic receptor. RT-PCR and Western blotting were used to confirm the presence of both PMCA and NHERF-2 in these cells. Cell surface biotinylations were performed to investigate the changes in levels of PMCA at the plasma membrane following activation of M3 receptor by acetylcholine (ACh). NHERF-2 contains 3 binding domains, PDZ-1, PDZ-2 and the C-terminus. We used GST-fusions of these domains as well as full length NHERF-2 to characterise the interaction between NHERF-2 and PMCA. These interactions were validated *in vivo* using co-immunoprecipitation with a polyclonal NHERF-2 antibody and subsequent Western blotting with a pan-PMCA antibody. To examine the functional role of NHERF-2, endogenous protein was knocked down by transfecting siRNA plasmids. Changes in intracellular Ca^{2+} were measured using FURA-2 in a microplate assay.

RT-PCR and Western blots confirmed that HT29 cells expressed both NHERF-2 and PMCA isoform 1 and 4 (n = 3). Importantly, we found that the levels of PMCA at the plasma membrane increased by 62 ± 12% (n = 3) within 1 min of exposure to ACh and returned to control levels within 3 min. GST-pulldown experiments in HT29 cell lysates clearly showed that PMCA interacted with the second PDZ module of NHERF-2 (n=4). Co-immunoprecipitation experiments using HT29 cell lysates confirmed the interaction between NHERF-2 and PMCA occurred under *in vivo* conditions (n=3). Silencing of NHERF-2 reduced the levels of endogenous NHERF-2 by a 68 ± 10% (n = 3). When we examined the Ca^{2+} response to ACh in the cells where NHERF-2 had been silenced we observed that the rate of recovery from the peak Ca^{2+} transient was 50 ± 10% (n = 3; $P < 0.05$) faster than in control cells.

These data reveal for the first time that the increase in intracellular Ca^{2+} in response to M3 receptor activation is accompanied by a rapid increase in PMCA at the plasma membrane, presumably due to translocation from subplasmalemmal stores. The functional interaction between NHERF-2 and PMCA may underlie the changes in recovery rate of Ca^{2+} following exposure to ACh. Further studies will provide new insights into how scaffold proteins may confer specificity in terms of G-protein mediated Ca^{2+} signalling.

Demarco, S., Chicka, M. & Strehler, E. (2003) *Journal of Biological Chemistry* **277**, 10506-11.
Pawson, T. & Scott, J. (1997) *Science* **278**, 2075-80.
Strehler, E. & Zacharias, D. (2001) *Physiological Reviews* **81**, 21-50.

NHERF1 - a novel scaffold protein for the astroglial glutamate transporter GLAST

A. Rayfield[1], A. Lee[1], D. Pow[2], D. Hryciw[1], T.A. Ma[1], S. Broer[3], C. Yun[4] and P. Poronnik[1], [1]School of Biomedical Sciences, University of Queensland, Brisbane, QLD 4072, Australia,[2] Department of Anatomy, University of Newcastle, NSW 2308, Australia,[3] Division of Biochemistry and Molecular Biology, Faculty of Science, Australian National University, Canberra, ACT 0200, Australia and [4]Department of Medicine, Emory University, Atlanta, Georgia 30322, USA.

The Na^+/H^+ exchanger regulatory factor (NHERF) proteins, NHERF1 and NHERF2 are renal epithelial PSD95/Dlg/ZO-1 (PDZ) domain containing proteins (Weinman *et al.*, 1995; Yun *et al.*, 1997). NHERF proteins contain two tandem PDZ domains (PDZ1 and PDZ2), which associate with specific C-terminal motifs of target peptides. NHERF proteins also contain a C-terminal region able to interact with the Ezrin-Radixin-Moesin (ERM) proteins which provides a link to the actin cytoskeleton.

While NHERF proteins have been extensively characterised in kidney and other tissues, very little is known regarding NHERF expression in the central nervous system (CNS) and its possible-binding partners in the CNS. Tissues used for immunohistochemical and biochemical analyses were isolated from euthanised adult Wistar rats, following procedures approved by the University of Queensland Animal Ethics Committee. In this study, we performed immunohistochemical characterisation of the cellular distribution of NHERF1 and NHERF2 in the adult rat brain. Immunohistochemistry was performed on adult rat brain sections using polyclonal antibodies specific for NHERF1 and NHERF2. Expression of NHERF1 was shown to be widespread in brain, most prominently in hippocampus, thalamus, choroid plexus and cerebellum. In these different regions of the brain, NHERF1 was primarily restricted to astrocytes. NHERF2 expression was primarily restricted to endothelial cells of blood vessels and capillaries. The distribution in adult rat brain was similar to that of GLAST, an astroglial glutamate transporter that also contains a potential PDZ binding consensus sequence (ETKM) in its COOH-terminus (Lehre, *et al.*, 1995). Double immunofluorescence labelling studies were performed using antibodies specific for GLAST and NHERF1 and imaged by confocal microscopy, co-localisation of GLAST and NHERF1 was detected in astroglial cells. Using solubilised adult rat brain lysate, co-immunoprecipitation experiments demonstrated that GLAST, NHERF1 and ezrin co-associate *in vivo*. To determine which domains of NHERF1 and GLAST interact we performed pull-down assays using solubilised adult rat brain lysate and GST-fusion proteins of the GLAST COOH-terminus, full-length NHERF1 and various domains of NHERF1 (PDZ1, PDZ2 and ERM domain). These experiments revealed that the GLAST-NHERF1 interaction requires the COOH-terminal ETKM sequence of GLAST and utilises the PDZ1 domain of NHERF1.

Therefore we have demonstrated that NHERF1 links GLAST to the actin cytoskeleton through ezrin, leading to the formation of a multi-protein complex. Linkage of GLAST to NHERF1 may serve as an important mechanism for localising the GLAST transporter to specialised membrane sites in astrocytes or for regulating transport activity.

Lehre, K P., Levy, L.M., Ottersen, O.P., Storm-Mathisen, J. & Danbolt, C.N. (1995) *Journal of Neuroscience* **15**, 1835-1853.

Weinman, E.J., Steplock, D., Wang, Y. & Shenolikar, S. (1995) *Journal of Clinical Investigation* **95**, 2143-2149.

Yun, C.H., Oh, S., Zizak, M., Steplock, D., Tsao, S., Tse, C.M., Weinman, E.J. & Donowitz, M. (1997) *Proceedings of the National Academy of Sciences of the United States of America* **94**, 3010-3015.

Molecular cloning and characterisation of the mouse ‘system IMINO’ transporter

S. Kowalczuk[1], A. Bröer[1], M. Munzinger[1], N. Tietze[1], K. Klingel[2] and S. Bröer[1], [1]School of Biochemistry & Molecular Biology, Australian National University, Canberra, ACT 0200, Australia and [2]Department of Molecular Pathology, University of Tübingen, 72076 Tübingen, Germany.

The SLC6 family consists of transporters for amino acids, neurotransmitters and osmolytes. These transporters play an important role in the removal of neurotransmitters in brain tissue and in amino acid transport in epithelial cells. The SLC6 family also contains a number of orphan transporters. Recently we identified a new member of the SLC6 family (B^0AT1 or SLC6A19), which is closely related to the orphan transporters and transports neutral amino acids. We hypothesized that other orphan transporters may be amino acid transporters as well.

To test this hypothesis we studied the mouse slc6a20 gene. The mouse has two homologues that correspond to single the human SLC6A20 gene, which are known as XT3 and XT3s1. RT-PCR analysis revealed expression of XT3s1 in the brain, kidney, small intestine, thymus, spleen and lung, while expression of XT3 was restricted to kidney and lung. Subsequently, we isolated full-length cDNA clones of XT3s1 and XT3 from brain and kidney, respectively. In situ hybridisation showed strong expression of XT3/XT3s1 in the proximal tubules of kidney cortex, in intestinal villi and in the brain.

Expression of mouse XT3s1, but not XT3, in Xenopus laevis oocytes induced Na^+- and Cl^--dependent transport of proline, hydroxyproline, glycinebetaine, MeAIB and pipecolic acid. Activation analysis suggests a $1Na^+/1Cl^-$/proline cotransport, which would be electroneutral. However, uptake experiments under voltage-clamp conditions suggest translocation of 1 charge per proline molecule. This apparent discrepancy can be explained by the very high affinity of the chloride binding site - chloride transport is likely to occur by way of an exchange process and thus will not affect the electrogenicity of the transporter.

The substrate specificity and mechanism of transport by XT3s1 fits well with the properties of the classical ‘system IMINO’, one of the major proline resorption systems of the intestine and kidney (Stevens & Wright, 1985). Together, the expression pattern and functional characteristics of SLC6A20 suggest a possible involvement in the inherited aminoaciduria iminoglycinuria.

Stevens, B.R. & Wright, E.M. (1985) *Journal of Membrane Biology* **87**, 27-34.

Increased acetaminophen hepatotoxicity in the NaS1 sulphate transporter null mouse

S. Lee, P.A. Dawson and D. Markovich, School of Biomedical Sciences, University of Queensland, Brisbane, QLD 4072, Australia.

Sulphate (SO_4^{2-}) plays an important role in the detoxification of numerous xenobiotics, including the widely used analgesic drug, acetaminophen (APAP) (Cole & Evrovski, 2000). The Na^+-SO_4^{2-} cotransporter, NaS1 is expressed in the kidney, where it maintains blood sulphate levels (Markovich, 2001). *NaS*1 knock-out (*Nas1*$^{-/-}$) mice exhibit hyposulphataemia and hypersulphaturia (Dawson *et al*. 2003). This project assessed the molecular, biochemical and physiological consequences of APAP challenge. Male *Nas1*$^{+/+}$ and *Nas1*$^{-/-}$ mice aged 1-4 months (*n*= 5-7 mice), were injected with 125-, 250- or 500-mg/kg of APAP i.p. The animals were sacrificed at various times (0, 2, 4, 5, 6 and 12 hours) after APAP administration. Serum alanine aminotransferase (ALT) levels in *Nas1*$^{+/+}$ and *Nas1*$^{-/-}$ mice were measured as an indicator of APAP-induced liver injury. ALT levels were 3-fold higher in *Nas1*$^{-/-}$ mice when compared to *Nas1*$^{+/+}$ mice at 12 hours after APAP treatment (250-mg/kg). This supports our histological findings of increased cellular damage in *Nas1*$^{-/-}$ mice. Extensive haemorrhaging was observed in lobular areas of *Nas1*$^{-/-}$ mice (500-mg/kg APAP, t=5 hours post-injection) but not in *Nas1*$^{+/+}$ mice. Hepatic glutathione (GSH) depletion was greater in *Nas1*$^{-/-}$ mice (87% reduction), compared to *Nas1*$^{+/+}$ mice (63% reduction) at 250-mg/kg dosage regime (t=2 hours post-injection) whereas repletion of GSH showed no significant differences between and *Nas1*$^{+/+}$ and *Nas1*$^{-/-}$mice. The GSTpi mRNA levels were significantly induced (2-fold) in *Nas1*$^{-/-}$ mice, when compared to *Nas1*$^{+/+}$ mice. The induction of GSTpi mRNA levels in APAP-treated *Nas1*$^{-/-}$ mice, could be a compensatory response to the GSH depletion. The mRNA levels of CYP3A11, which are responsible for the production of reactive metabolite, *N*-acetyl-*p*-benzoquinone imine (NAPQI) (Zhang *et al.*, 2002), were significantly increased (1.5-fold) in *Nas1*$^{-/-}$ mice when compared to *Nas1*$^{+/+}$ mice (250-mg/kg APAP, t=2 hours post-injection). In summary, we have identified increased APAP-induced hepatotoxicity and more rapid GSH depletion in the hyposulphataemic *Nas1*$^{-/-}$ mice and this may be due to low blood sulphate levels, which limits APAP sulphonation. This study suggests the potential role of NaS1 in the modulation of APAP-induced hepatotoxicity.

Cole, D.E. & Evrovski, J. (2000) *Critical Reviews in Clinical Laboratory Sciences* **37**, 299-344.

Dawson, P.A., Beck, L. & Markovich, D. (2003) *Proceedings of the National Academy of Science U.S.A.* **100**, 13704-13709.

Markovich, D (2001) *Physiological Reviews* **81**, 1499-1534.

Zhang, J., Huang, W., Chua, S.S., Wei, P. & Moore, D.D. (2002) *Science* **298**, 422-424.

The influence of dietary fish oil and exercise upon oxidative status biomarkers in a rat model

R. Henry, A.J. Owen and P.L. McLennan, Smart Foods Centre, Department of Biomedical Science, University of Wollongong, NSW 2522, Australia.

Introduction. Oxidative stress is implicated in cardiovascular and many other diseases, as well as in normal aging. Highly unsaturated omega-3 fatty acids are very susceptible to oxidation and the generation of reactive oxygen species while intense exercise promotes an environment for increased oxidation. Paradoxically, both chronic dietary fish oil consumption and chronic exercise are associated with reduced cardiovascular disease morbidity and mortality.

Objective. This study aimed to determine the effect of dietary fish oil and exercise training on membrane fatty acid composition and biomarkers of oxidative stress in tissues representative of different levels of oxidation.

Methods. Male Wistar rats, fed either saturated fat (SF) or fish oil (FO) diets for 6 weeks were exercise trained (weighted swimming, 1h/d, 5d/w with 2% body weight on tail) or remained sedentary. Rats rested for 2 days and fasted overnight were anaesthetised (pentobarbitone sodium 60mg/kg i.p) and killed by rapid exsanguination. Liver and skeletal muscles (diaphragm, abdominal sheath and white vastus lateralis) were analysed for membrane fatty acids, lipid peroxidation products and endogenous antioxidants: glutathione peroxidase and superoxide dismuatse.

Outcomes. In all tissues FO feeding increased EPA, DHA, total n-3 PUFA and the unsaturation index and decreased arachidonic acid, total n-6 PUFA and n-6/n-3 ratio ($p<0.05$). Exercise training increased membrane arachidonic acid ($p=0.023$) in the FO liver but decreased DHA($p=0.002$) and total n-3 PUFA ($p=0.017$) compared to FO sedentary. The liver compared to muscle tissue and diaphragm compared to other muscles had higher membrane arachidonic acid (AA) and lower DHA content. Lipid hydroperoxidation varied according to tissue phospholipid unsaturation but there was no additional effect of fish oil consumption or exercise training. Activities of glutathione peroxidase and superoxide dismutase varied according to tissue metabolic activity (liver >> muscle (diaphragm > abdominal muscle)) with no additional effect of fish oil consumption or exercise training.

Conclusion. Fatty acid composition and antioxidant enzyme activity may be related to the oxidative functions of different tissues. Despite incorporation of n-3 PUFA into cell membranes, fish oil feeding did not increase tissue oxidative stress measured at rest and exercise training was not associated with altered oxidative stress biomarkers at rest.

Simulation of visual processing in retinal ganglion cells

M. Watson,[1] G. Holmes,[1] T. Byrne[2] and S. Cornford,[1] [1]Department of Biological & Physical Sciences, Faculty of Sciences, [2]Faculty of Engineering and Surveying, University of Southern Queensland, Toowoomba, QLD 4350, Australia.

The retina contains photoreceptors for light detection as well as bipolar, horizontal, amacrine and ganglion cells. These form a neural network where synaptic convergence, divergence and integration take place. It serves as a simple network to simulate and thus can be used as a learning tool to demonstrate neural processing, desensitization, experimental design and protocol. The simulation is designed for students to facilitate inquiry based learning.

A given retinal ganglion cell responds to light directed to a specific area of the retina. This area is called the 'receptive field'. Ganglion cell receptive fields have a 'centre' and an antagonistic 'surround' and can be classified as 'On Centre' or 'Off Centre'. On Centre are activated by light in the centre of the receptive field and inhibited by light in the surrounding receptive field. Off Centre are inhibited by light in the centre of the receptive field and activated by light in the surrounding receptive field.

The model simulates the receptive fields of four ganglion cells. The four receptive fields are arranged into 4 arrays with each array containing 64 Light Dependent Resistors (LDR's; EG&G Vactec). These simulate the photoreceptors contained within each receptive field. The LDR's are connected *via* the Multiplexor (Temic) and through the programming of a HC12 microprocessor (Motorolla) simulate the 'On Centre' and 'Off Centre' receptive fields.

Students shine a variable point of light onto one of the four array's and will see either an increase or decrease in the clock rate output of the HC12. This represents a change in the discharge of the ganglion cell. The clock rate output of the HC12 is visualised by means of an oscilloscope. The clock rate output will vary depending on whether they are activating 'On' or 'Off' LDR's. Prolonged stimulation of the LDR's reduces the clock rate output to pre- stimulus levels to simulate desensitization.

Students are required to design an experimental protocol that determines an optimal standard stimulus, a systematic protocol for testing the different receptive fields and a protocol for gathering and analysing the data. The simulation challenges students to determine: (i) the optimum size, strength and duration of a stimulus that is sufficient to stimulate the receptive field; (ii) the receptive field characteristics of retinal ganglion cells; (iii) how such receptive fields can be formed on the basis of the cell types and connections found in the retina.